

AN ABSTRACT OF THE THESIS OF

Paul Robert Crowley for the degree of Master of Science in Radiation Health
Physics presented on January 14, 2000. Title: Behavior of ^{59}Fe in a Marine
Estuarine Environment: Uptake and Retention by the Pacific Basket-Cockle,
Clinocardium nuttallii.

Redacted for Privacy

Abstract approved: _____

Kathryn A. Higley

Iron-59 and its speciation in a cold model estuary were chosen as the focus for this study on the effects and behavior of radionuclides in the marine environment. Iron-59 is a common constituent of the reactor effluent water found on U. S. Naval, nuclear powered warships. It could provide useful data in assessing the radiological impact of shipborne reactor accident resulting in the release of radionuclides to the marine estuarine environment.

As sedimentary filter feeders, bivalves act as excellent bioindicators for marine contamination. *Clinocardium nuttallii*, Pacific basket-cockles, were maintained in a recirculating chilled-seawater aquarium. All specimens, seawater and sediment were extracted from Yaquina Bay in Newport, Oregon. After allowing the organisms to acclimate to the laboratory conditions, 1.0 mCi of ^{59}Fe was added to the system in aqueous form as iron (III) chloride and allowed to homogeneously distribute. Over a twenty-one day period, or one half of one half-

life for ^{59}Fe , frequent water, sediment, and cockle samples were drawn, weighed and counted for activity in a sodium iodide, NaI(Tl), solid scintillation detector. All specific activity measurements were corrected for radioactive decay and plotted vs. time after iron introduction to determine the iron speciation pathways within the system. At the end of the data collection period, five cockles removed from the system at various times during the experiment were dissected for a tissue distribution study.

The results show that ^{59}Fe rapidly binds to suspended particulate in the water column, and within a few days, most of the iron added to the system was associated with the bottom sediment layer. During the first few days, while suspended particles filtered down through the water column, the cockles fed actively and assimilated ^{59}Fe at a fairly high rate. These results confirm previous bivalve studies suggesting filter-feeding as the primary means for radionuclide uptake. Laboratory and time constraints as well as sampling inconsistencies limited the ability of this experiment to satisfactorily meet all objectives. No convincing evidence was found for: (1) sediment-to-seawater transfer of ^{59}Fe ; (2) retention of ^{59}Fe by *Clinocardium nuttallii*; (3) tissue distribution patterns for ^{59}Fe in *Clinocardium nuttallii*. Future research is needed in these areas to more accurately establish and predicate the behavior of ^{59}Fe under varying marine conditions; however, this experiment successfully establishes sedimentation patterns and uptake mechanisms for ^{59}Fe in the marine estuarine environment.

©Copyright by Paul Robert Crowley
January 14, 2000
All Rights Reserved

Behavior of ^{59}Fe in a Marine Estuarine Environment:
Uptake and Retention by the Pacific Basket-Cockle, *Clinocardium nuttallii*

by

Paul Robert Crowley

A THESIS

submitted to

Oregon State University

in partial fulfillment of
the requirements for the
degree of

Master of Science

Presented January 14, 2000
Commencement June 2000

Master of Science thesis of Paul Robert Crowley presented on January 14, 2000

APPROVED:

Redacted for Privacy

Major Professor, representing Radiation Health Physics

Redacted for Privacy

Chair of Department of Nuclear Engineering

Redacted for Privacy

Dean of Graduate School

I understand that my thesis will become part of the permanent collection of Oregon State University libraries. My signature below authorizes release of my thesis to any reader upon request.

Redacted for Privacy

Paul Robert Crowley, Author

ACKNOWLEDGEMENTS

The completion of this work would not have been possible without the assistance of the following people: Capt. Marvin Rice, USN (Ret.) and Capt. Thomas Daniels, USN, who convinced me of the importance of this undertaking and provided me the latitude and encouragement to see it through to the end; Larry Tyler, who designed and built a superb cold water marine aquarium with which to conduct my experiments and provided valuable assistance on its maintenance and upkeep; Oleg Povetko, who shared his laboratory space and his knowledge of laboratory procedures and instrument calibration, without which I would still be cursing all things electronic; Mark Treen, my laboratory assistant, whose patience and computer skills proved vital during the experimental stage of this project; Dr. Robert Collier, professor of chemical oceanography and my minor professor, who provided me with a reality check in the world of marine biochemistry and estuarine processes.

A special thank you is extended to Sherry West, aquarist for the Hatfield Marine Science Center. Her assistance and guidance in the collection and maintenance of marine organisms was impressive. Braving the winds and wet winter cold to dig up cockles and worms went far beyond the call of duty. I will remain forever in your debt.

A special note of appreciation must go to my major professor Dr. Kathryn Higley, who patiently saw me through the entire research and degree process. Her

practical advice and encouragement helped steady me on the oft-wandering path I wove to completion of this project. She showed patience in accommodating my undergraduate shortcomings and full-time employment and inspired me to think for myself instead of choosing the "easier" path.

Special recognition, of course, must go to my wife Salome and to my family. Without their help, which ranged from accompanying me on clam digging trips and water collection to proofreading rough drafts, I would have suffered mightily in completing my work (thanks even to Moose and Ollie for keeping those pesky seagulls from stealing our catch). Their support, patience, and encouragement, especially down the homestretch, were integral contributions to the successful completion of this degree.

TABLE OF CONTENTS

	<u>Page</u>
INTRODUCTION	1
Iron	2
Sources of Radioactive Iron in the Marine Environment	3
Behavior of ^{59}Fe in the Marine Environment	4
Bivalves as Bioindicators	5
The Pacific Basket – Cockle	6
Taxonomy	6
Filter Feeding Mechanisms	10
Objectives of this Study	14
MATERIALS AND METHODS	17
Radioisotope	17
Counting System	18
Marine Ecosystem	23
Sample Collection and Maintenance	26
Laboratory Experiment	30
RESULTS	34
Sediment	34
Water	37
Bivalves	42
Tissue Distribution Study	48

TABLE OF CONTENTS (Continued)

	<u>Page</u>
DISCUSSION	51
Iron Speciation	52
Uptake and Retention by <i>Clinocardium nuttallii</i>	55
CONCLUSIONS	57
Summary	57
Recommendation for Future Research	58
BIBLIOGRAPHY	60
APPENDIX	64

LIST OF FIGURES

<u>Figure</u>	<u>Page</u>
1. A cockle, <i>Cardium</i> sp., in its normal feeding position	8
2. Lateral view and cross section view through the shell of a bivalve	8
3. Burrowing sequence of a cockle	9
4. Internal anatomy of a bivalve	13
5. The digestive system of a suspension-feeding lamellibranch bivalve	15
6. A lamellibranch bivalve gill	15
7. Detector calibration PLOT – total counts vs. LLD setpoint	20
8. Optimum LLD Setting vs. gamma energy plot	21
9. Yaquina Bay, Oregon	24
10. Chilled-seawater aquarium schematic drawing	25
11. Photograph of Yaquina Bay tidal flats	27
12. Sediment - specific count rate plot (activity decay corrected)	35
13. Sediment mean specific count rate plot (activity decay corrected)	36
14. Water specific count rate plot (activity decay corrected)	38
15. Water mean specific count rate plot (activity decay corrected)	39
16. Sump tank water specific count rate plot (activity decay corrected)	41
17. Cockle specific count rate plot 1 (activity decay corrected)	43
18. Cockle specific count rate plot 2 (activity decay corrected)	44
19. Cockle specific count rate plot 3 (activity decay corrected)	45

LIST OF FIGURES (Continued)

<u>Figure</u>	<u>Page</u>
20. Cockle mean specific count rate plot (activity decay corrected)	46
21. Tissue distribution sample count rate plot (activity decay corrected)	49

LIST OF APPENDIX TABLES

<u>Table</u>	<u>Page</u>
1. Sediment sample count rate data	65
2. Surface water sample count rate data	68
3. Deep water sample count rate data	70
4. Bottom (interstitial) water sample count rate data	72
5. Sump tank water sample count rate data	74
6. Cockle (<i>Clinocardium nuttallii</i>) sample count rate data	75
7. Retention experiment sample data	79
8. Bent-nose clam (<i>Macoma nasuta</i>) sample count rate data	80
9. Tissue distribution sample count rate data	81

Behavior of ^{59}Fe in a Marine Estuarine Environment: Uptake and Retention by the
Pacific Basket-Cockle, *Clinocardium nuttallii*

INTRODUCTION

Knowledge of the behavior of radionuclides in the marine environment is of considerable importance when attempting to assess the potential radiological impact of radionuclide releases. The environmental presence of radioactive iron isotopes as a result of nuclear weapons testing and the nuclear fuel cycle has been known for quite some time [NAS, 1971; Burton, 1975]; despite this, surprisingly limited research has been undertaken to investigate its environmental and radiobiological impact. Iron is of interest in the study of marine ecosystems because it is such an important metabolic element and is not found in great quantities in the ocean. One specific isotope of iron, ^{59}Fe , is of particular interest, due to its relative abundance in reactor effluent water and its rapid sorption on sediment and suspended particulate matter. This study then, has been undertaken in order to add to the body of knowledge concerning the behavior of radioactive iron in the marine environment, specifically in the seawater-sediment interface of an estuarine ecosystem.

Iron

The chemical element, iron (Fe), has been known since ancient times, with identified smelted iron artifacts dating as far back as 3000 BC. The name "iron" originates from the Anglo-Saxon word "iron" and its chemical symbol comes from the Latin word "ferrum" meaning iron.

Iron is a first row transition element, with an atomic number of 26 and atomic mass of 55.845 AMU. Iron has four stable isotopes, and its most common radioactive isotopes are ^{55}Fe , with a 2.73 year half-life, and ^{59}Fe , with a 44.51 day half-life [Eisenbud and Gesell, 1997]. Iron has a 2,000 day biological half-life in humans. Iron is a fairly reactive metal, found principally in compounds in one of two oxidation states: +2 and +3. Iron (II) is easily oxidized to iron (III), which is the thermodynamically stable form of iron in an oxic marine environment.

Radioactive iron, ^{59}Fe , is produced when the relatively rare iron isotope, ^{58}Fe (just 0.28% abundant in nature) captures a thermal neutron by the reaction, $^{58}\text{Fe}(n,\gamma)^{59}\text{Fe}$. Iron-59 undergoes radioactive decay by beta particle emission, releasing energy in the form of gamma rays and beta particles as it decays to the stable isotope, ^{59}Co . Iron-59 can also be produced from beta decay of ^{59}Mn , but this rarely occurs outside of the laboratory environment. It releases two common beta particles, with energies of 466 (53.1% probability) and 273 (45.2%) keV; and, it also releases two common gamma rays, with energies of 1.099 (56.5 %) and 1.292 (43.2%) MeV [Schleien, 1992].

Sources of Radioactive Iron in the Marine Environment

Iron is the second most abundant metal and fourth most abundant element in the earth's crust (~5% by weight) [Brady and Humiston, 1982]. In its natural form, it is most commonly incorporated as silicate, oxide, or sulfite bound minerals of low solubility, with measured concentrations varying from 35.4 mg Fe per g of upper Continental crust magmatic rocks to 56.3 mg Fe per g of igneous rock [Coughtrey and Thorne, 1983]. Only trace amounts of radioactive iron can be found naturally in these ores.

Man-made sources account for the vast majority of radioactive iron in the marine environment. Nuclear weapons testing has produced the widest distribution of radioactive iron in the marine environment. Both ^{55}Fe and ^{59}Fe are produced as activation products during detonation and are dispersed with the prevailing winds. Nuclear power plants and reprocessing facilities provide a second source of radioactive iron to the marine environment. ^{59}Fe is a common corrosion product found in reactor effluent water, with typical concentrations of 5.1×10^{-4} microcuries per milliliter ($\mu\text{Ci/ml}$) found in U. S. Navy nuclear reactor primary coolant waters [NAS, 1971]. With the cessation of above ground nuclear weapons testing in the 1960s and the relatively short half-lives of both common radioactive iron isotopes, this study concentrates on the latter mode of introduction to the marine environment.

On January 17, 1955, *USS Nautilus* (SSN 571) put to sea for the first time and ushered in a new age of naval warfare, signaling her historic message:

"Underway on nuclear power." Today, the United States Navy's operational fleet includes seventy vessels propelled by nuclear power. These aircraft carriers and submarines comprise eighty-five, pressurized water nuclear reactors stationed at sea and in ports across the globe. The Naval Nuclear Propulsion Program has been a forerunner in the effort to recognize the environmental aspects of nuclear power. Through the entire history of the program, over 5000 reactor years of operation and over 114 million miles steamed on nuclear power, there has never been a reactor accident, or any release of radioactivity that has had a significant effect on the public or the environment [DOD/DOE, 1998]. Despite this impressive safety record, the potential for a significant radiological incident cannot be ignored. With nuclear powered vessels moored in unique marine and estuarine ecosystems such as Puget Sound, the Chesapeake Bay, and the Thames River in New London, CT, a significant release of radionuclides to the environment could have a profound impact on these diverse habitats.

Behavior of ^{59}Fe in the Marine Environment

Because ^{59}Fe generally enters the marine environment through aqueous pathways, it is more bioavailable and readily cycled than the majority of stable iron found naturally in the marine environment. Iron-59 is most prevalent as hydrolyzed Fe-III in seawater at a typical pH of 8.1. In an oxidizing environment, it is readily precipitated as $\text{Fe}(\text{OH})_3$, but has subsequently been found to be as easily released from the sediment to the water in a reducing environment. When

soluble iron compounds are added to seawater, 70% of the total can be expected to be bound rapidly to suspended particulate via irreversible binding processes. Of the 30% that remains in solution, 60% can be expected to be present as Fe^{3+} and 40% to be in association with organic compounds [Coughtrey and Thorne, 1983]. This differs markedly from observations of stable iron of which >99% is incorporated in suspended sediments. This higher solubility leads to an observed increase in the bioavailability of radioactive iron as compared to stable iron, and the higher solubility tends to be magnified in more acidic waters [Burton, 1975].

Bivalves as Bioindicators

Due to the complexity of physical processes as well as the rapid transformation and cycling times of pollutant elements in the ocean, it is often difficult to get an accurate assessment of the radioecological impacts of a radionuclide release to the marine environment. The key to successful radioecological impact assessment is the selection and rapid sampling of bioindicators. When selecting indicator organisms, occurrence, ease of sampling, endurance of the organisms in changing environmental conditions and the ability to accumulate one or more radionuclides should be considered [Paakkola, 1994]. Bivalves have been shown to be effective concentrators of trace elements and thus have proved useful as indicators of radioactive contamination by radioactive trace elements [Young and Folsom, 1972; Evans, 1984; Hamilton *et al.*, 1991; McDonald *et al.*, 1993a; Dahlgaard, 1994].

Bivalves are relatively sessile and are often representative of the region in which they were collected for many years. McDonald *et al.* (1993a, 1993b) were able to estimate human population doses from shellfish consumption in the Cumbrian region of the United Kingdom, by collecting and sampling mussels (*Mytilus edulis*) and winkles (*Littorina littorea*) contaminated by alpha-emitting transuranic radionuclides discharged to the Irish Sea over a forty year period by the nuclear fuel reprocessing plant near Sellafield. Fish and plankton, on the other hand, are motile organisms that may cycle in and out of the region of interest on a fairly continuous basis.

Bivalves are quite abundant in coastal marine environments and have also been shown to be able to thrive in the laboratory under a variety of environmental conditions [Shimizu, 1975]. Additionally, bivalves have been shown to accumulate ^{59}Fe in both natural and laboratory conditions [Pentreath, 1973; Coimbra and Carraça, 1990; Allison *et al.*, 1998]. Filter-feeding bivalves are especially suited for iron contamination studies because they process the seawater and suspended particulate matter near the water-sediment interface where the bulk of radioactive iron has been shown to accumulate.

The Pacific Basket – Cockle

Taxonomy

The Pacific basket-cockle, or heart cockle, was so named for its “heart-shaped” shells. Its present nomenclature, *Clinocardium nuttallii*, developed

through a series of marine investigations and reclassifications. The first American categorization of the species was by T. A. Conrad in 1837, who described this species along with other *Cardium* species of the West Coast of the United States. His description came from a collection of marine shells belonging to Thomas Nuttall [Ratti, 1977]. The genus, *Clinocardium* (which means literally, sloping heart), is attributed to A. M. Keen, who categorized some eighty-nine species of the family *Cardiidae* along the western boundary of the Americas. The present taxonomic classification of *Clinocardium nuttallii* is as follows [Kozloff, 1987]:

Phylum Mollusca
 Class Bivalvia
 Subclass Heterodonta
 Order Veneroida
 Family Cardiidae
 Genus *Clinocardium* Keen, 1936.
 Species *nuttallii* Conrad, 1837

Clinocardium nuttallii is a common species of bivalve found in intertidal and shallow subtidal zones along the Eastern Pacific coast from the Gulf of Alaska to Baja California. It does not constitute a major economic resource for the marine fisheries industry but remains a popular catch of sport diggers [Marriage, 1958]. *Clinocardium nuttallii* are occasionally found entirely exposed on the surface of the sediment, but they are active animals and can dig in quickly with their large feet. They burrow, shallowly however, for their siphons are little more than openings in the margin of the mantle [Ricketts, 1985] (Fig. 1).

The heart cockle shares many attributes with other species in the bivalve class (Fig. 2). It possesses a shell with two valves joined together dorsally

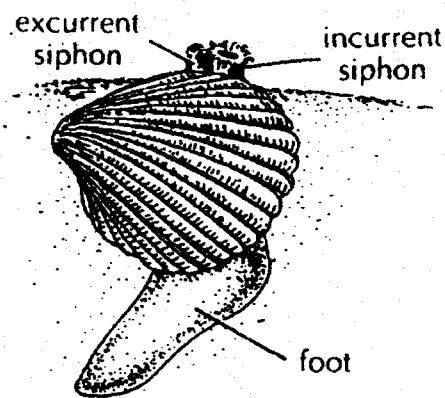


Figure 1. A cockle, *Cardium* sp., in its normal feeding position. From Pechenik (1996). Copyright © 1996 by Times Mirror Higher Education Group, Inc., New York. Reprinted by permission of The McGraw-Hill Companies.

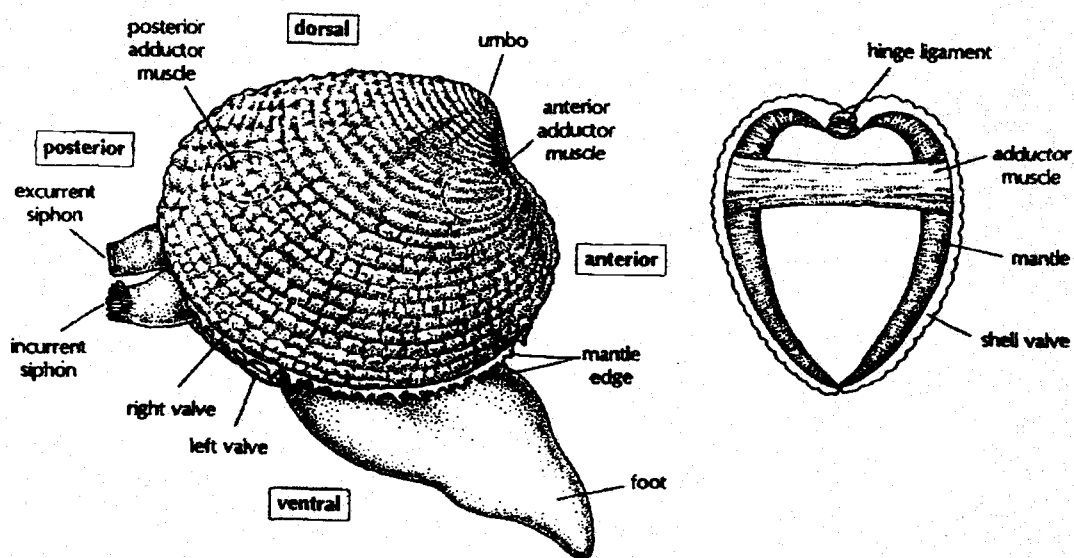


Figure 2. Lateral view and cross section view through the shell of a bivalve. From Pechenik (1996). Copyright © 1996 by Times Mirror Higher Education Group, Inc., New York. Reprinted by permission of The McGraw-Hill Companies.

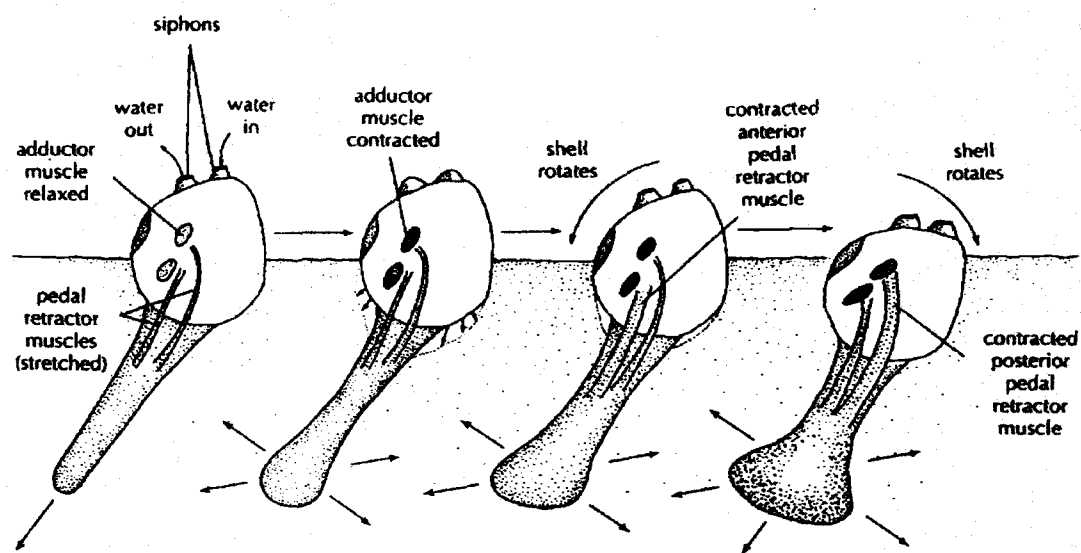


Figure 3. Burrowing sequence of a cockle. From Pechenik (1996)., Copyright © 1996 by Times Mirror Higher Education Group, Inc., New York. Reprinted by permission of The McGraw-Hill Companies.

(left and right) by a hinge ligament that acts to spring the valves apart under relaxed conditions. Posterior and anterior adductor muscles enable the cockle to close the two valves. The heart cockle possesses a large mantle cavity and very large gills, which have assumed a food collecting function in addition to that of gas exchange, and it is remarkable in the virtual absence of a head and associated sensory structures [Pechenik, 1996]. Its foot, like the rest of its body is laterally compressed, giving the origin of the name Pelcypoda – hatchet foot [Barnes, 1980]. This foot can be used defensively as a thruster to escape predators and is also used in burrowing to first penetrate the substrate and then serve as an anchor while the rest of its body is pulled downward [Barnes, 1980; Newell, 1979] (Fig. 3).

Filter Feeding Mechanisms

In order to understand uptake of radionuclides by marine bivalves, it is important to discuss the mechanism by which they process water and suspended material in an effort to satisfy their metabolic needs. This process is referred to as filter feeding, and it is an adaptation that enables bivalves to feed on suspended microscopic food particles that cannot be immediately sensed and seized [Jørgensen, 1990]. In the filter feeding process, ambient water is drawn through filters (gills) that retain suspended matter, usually regardless of whether the material is organic or not. The rate of water filtration varies with different environmental parameters: temperature, seasonality in primary production, seston (inorganic) loading of the water column, contaminant loading, as well as others. In

general, suspension feeders will balance the high-energy cost of the filtering process with the organic content of suspended material in the water column. This is accomplished by filtering at a higher rate when phytoplankton stocks are low. They have also been shown to have a feeding threshold, a phytoplankton concentration below which they will not feed. Adult cockles are capable of processing as much as 25 liters of seawater per hour [Navarro and Iglesias, 1992]. With such a high filtration rate capability, a large community or bed of suspension feeders can have a significant impact on the estuarine ecosystem. Continuous feeding can graze down ambient phytoplankton stocks, deplete oxygen from the water column, and affect nutrient loading through biodeposition of feces and pseudofeces (rejected particulate matter) [Jørgensen, 1990].

Clinocardium nuttallii is well adapted to the mechanism of suspension filter feeding. High coastal phytoplankton concentrations and bottom material resuspended by tide and wind driven water movement mark the water column in its intertidal and shallow subtidal habitats. This resuspended material is largely inorganic in composition, but does comprise some particles of food value as well: detritus, benthic microfauna, and bacteria. While increasing the total concentration of particulate organic matter, this process also normally produces a dramatic decrease in particle quality with respect to the organic content of the suspended material [Navarro and Iglesias, 1992]. The filter feeding process enables the heart cockle to "process" the water for particles of high energy content [Barnes, 1990].

During the filter feeding process (Fig. 4), water enters and exits the mantle cavity posteriorly; the water enters through an incurrent siphon, passes dorsally between adjacent gill filaments, and then exits through a more dorsally located excurrent siphon [Pechenik, 1996]. Cockles have developed enlarged comb-like gills, ctenidia, when compared to many other bivalves, and this provides them with an enormous surface area for collecting, sorting, and transporting suspended particles. The gills are folded into a complex arrangement to maximize surface area, and water is forced through minute holes, ostia, in order to pass between gill filaments (Fig. 5). Lateral cilia along the sides of the gill filaments create the water currents responsible for moving water into, and out of, the mantle cavity.

The details of particle capture and transport by bivalve gills is still not fully understood. Jørgensen (1990, 1996) favors a mechanism by which physical constraints on feeding, such as viscosity of the medium and frictional forces influencing low Reynolds number flow within the mantle cavity, dominate filtration rate. Bayne (1993) and Navarro and Iglesias (1992) argue that behavioral and physiological processes largely determine feeding behavior. By which ever of these mechanisms a specific food particle is captured, it is moved by the frontal cilia to specialized food grooves located at the ventral and dorsal margins of each demibranch gill (Fig. 5). Periodically, *Clinocardium nuttallii* will close its valves forcefully, expelling water and unwanted food particles (pseudofeces) from the mantle cavity through the incurrent siphon [Barnes, 1980].

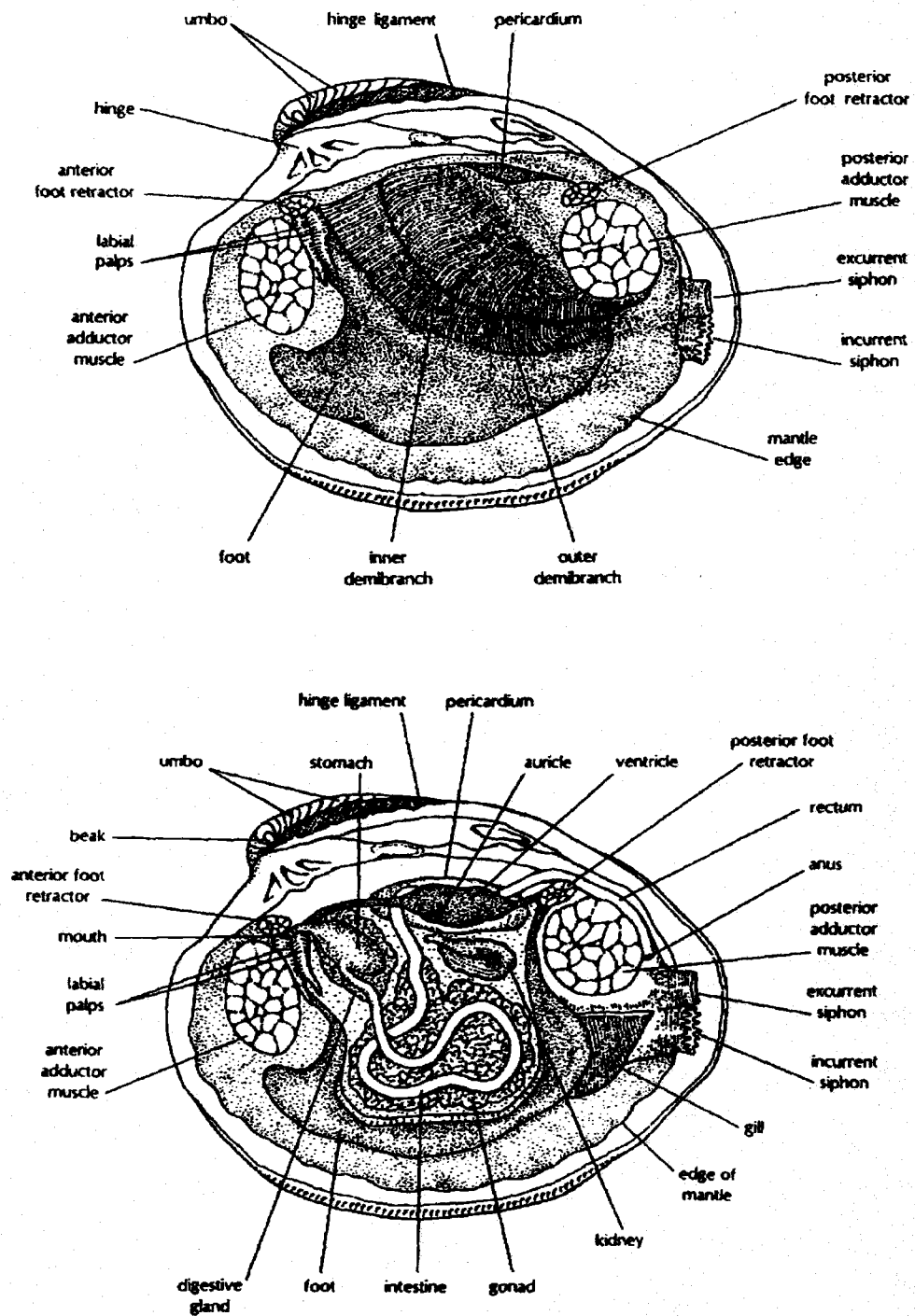


Figure 4. Internal anatomy of a bivalve. From Pechenik (1996). Copyright © 1996 by Times Mirror Higher Education Group, Inc., New York. Reprinted by permission of The McGraw-Hill Companies.

Particles are passed down the esophagus, entangled in strings of mucus, and then drawn into the stomach. Here they are stirred and, in part, digested by the action of a rotating translucent rod, the crystalline style (Fig. 6). The crystalline style is composed of structural protein and several digestive enzymes. It is rotated by cilia lining a pouch of the intestine that encompasses the anterior end of the crystalline style. The rotating action and friction between the crystalline style and the gastric shield act to break up particles and release digestive enzymes to the stomach [Barnes, 1980].

Objectives of this Study

The general objective of this study was to examine the behavior of ^{59}Fe in the marine estuarine environment under experimental conditions. Items specifically examined included:

- degree and rate of transfer of iron from its aqueous form to sediment, suspended particulate, and organisms in an experimental marine system
- degree and pattern(s) of whole-body iron accumulation by *Clinocardium nuttallii*
- pattern(s) of whole-body iron elimination by *Clinocardium nuttallii*
- estimates of concentration ratios and biological and effective half-lives for iron in *Clinocardium nuttallii*
- pattern(s) of tissue distribution of iron during uptake and elimination by *Clinocardium nuttallii*

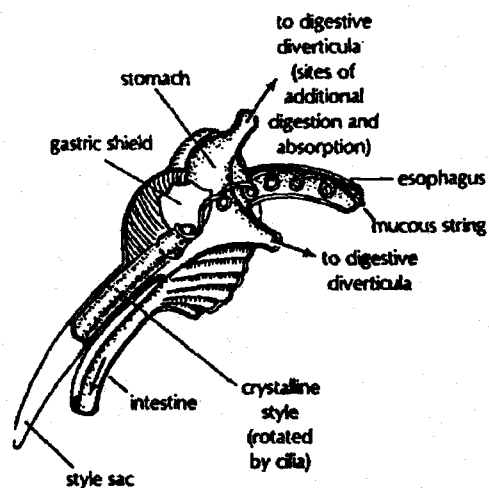


Figure 5. The digestive system of a suspension-feeding lamellibranch bivalve. *From Pechenik (1996). Copyright © 1996 by Times Mirror Higher Education Group, Inc., New York. Reprinted by permission of The McGraw-Hill Companies.*

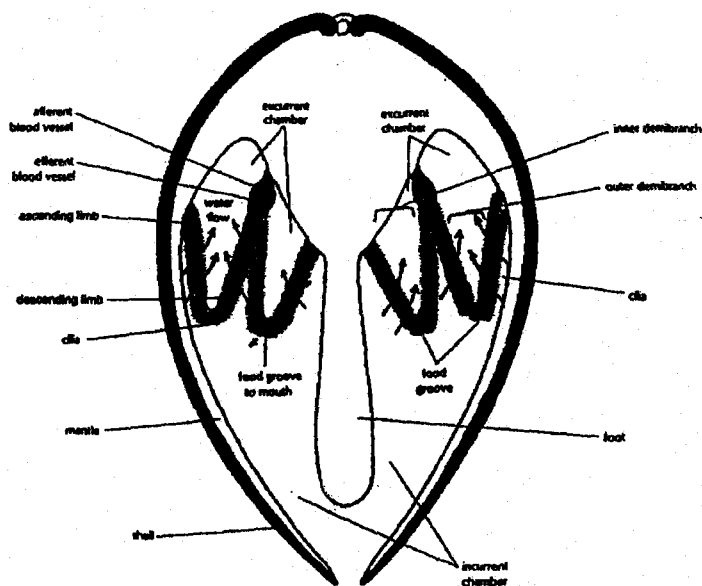


Figure 6. A lamellibranch bivalve gill. *From Pechenik (1996). After W. D. Hunter, A Life of Invertebrates. Copyright © 1979 by Macmillan Publishing Company, New York. Reprinted by permission of Macmillan Press Ltd.*

The data could then be used to make a preliminary assessment of the potential radioecological significance of a release of ^{59}Fe into a natural estuarine environment.

MATERIALS AND METHODS

Radioisotope

Iron-59 was used as a radiotracer in this study because it is a common corrosion product found in reactor effluent water. As such, it would provide useful data in assessing the impact of a naval reactor incident resulting in release of primary coolant water to the marine environment. Its 44.5 day half-life is short enough to allow for decay in storage and subsequent release of the laboratory equipment and contaminated waste products. Its half-life is long enough to minimize the impact of necessary radioactive decay adjustments on radioassay measurements for the relatively short duration of sampling. Additionally, iron's metabolic utility and previously established tendency to adsorb to suspended particulate material in the marine environment, make it especially suitable for a study of seawater-sediment interface.

An aliquot of ^{59}Fe , delivered as iron (III) chloride in a 0.1M HCl solution, was ordered through Amersham Pharmacia Biotech. The sample was assayed to contain 1.0 mCi at 8:00 AM on 01 April 1999. The aliquot contained 0.37 ml of solution with an iron concentration of 440 $\mu\text{g/ml}$. The solution was prepared for the experiment by transferring the contents of the aliquot using a filtered seawater flush and 5 ml pipette to a 25 ml volumetric flask. Filtered seawater collected from the Hatfield Marine Science Center was added to the stock to create a 25.0 ml sample solution for the study.

Counting system

A three inch diameter, sodium iodide, NaI(Tl), solid scintillation detector was used to radioassay all samples. A scintillation detector was chosen because of its moderate energy discrimination and gamma count yield characteristics. The detector was placed in a horizontal position shielded on all sides by two-inch thick lead bricks. This arrangement was selected to provide greater stability for the detector and the lead shield enclosure. Samples were placed on a lead brick, such that they were level and directly opposite the face of the detector. Because ^{59}Fe emits two strong beta particles, an 8 mm thick plastic shield was placed between the detector face and the sample to allow for exclusive gamma photon counting. Photons that react inside the crystal produce a signal which is then transmitted to a series of instruments housed in a NIMbin power supply designed to amplify, analyze and compute the output of the detector. A single channel analyzer (SCA) was used to isolate the ^{59}Fe gamma photons for counting.

To calibrate the detector, characteristic curves for the photomultiplier tube (PMT) were plotted using plastic ^{60}Co , ^{137}Cs , and ^{133}Ba sources. Photomultiplier tube output can vary depending on the high voltage level supplied to it. To minimize the effect of minor voltage fluctuations from the source power supply; a characteristic curve is plotted for the PMT to determine the plateau, a range of voltage setpoints, where associated count rates remain relatively steady. After determining the counting threshold potential for each source, high voltage supply to the detector was raised in 50 V increments, and each sample was counted. The

total counts were plotted against the voltage on a log-linear graph, and from the resulting plateaus, an optimum high voltage power supply (HVPS) setting of 1100 V was determined.

With the HVPS set to this voltage, the cesium and cobalt sources were used together to plot a gamma spectrum. The sources were counted by increasing the lower level discriminator (LLD) in 0.1 V increments with a 0.2 V window. The total absorption peaks for each gamma photon were determined from a plot of LLD setpoint versus total counts (Fig. 7). LLD settings were then estimated for the two common gamma photons emitted by ^{59}Fe using a straight-line approximation of the gamma spectrum plot (Fig. 8).

As no ^{59}Fe standard was available, a nominal "counting standard" was prepared. 1.0 ml of the sample solution was transferred to a container and diluted with 24.0 ml of filtered seawater. The total absorption peaks as predicted above were then checked using this standard. From this measurement, the total absorption peak corresponding to the more prevalent 1.1 MeV gamma photon was selected at an LLD setting of 5.2 V with a 0.3 V window.

The counting standard was counted for twenty seconds in the detector using the LLD settings determined above. This measured count rate was then compared to the actual activity of the sample to determine intrinsic detector efficiency. Intrinsic efficiency (E) is defined as:

$$E = C / (A \times \Omega)$$

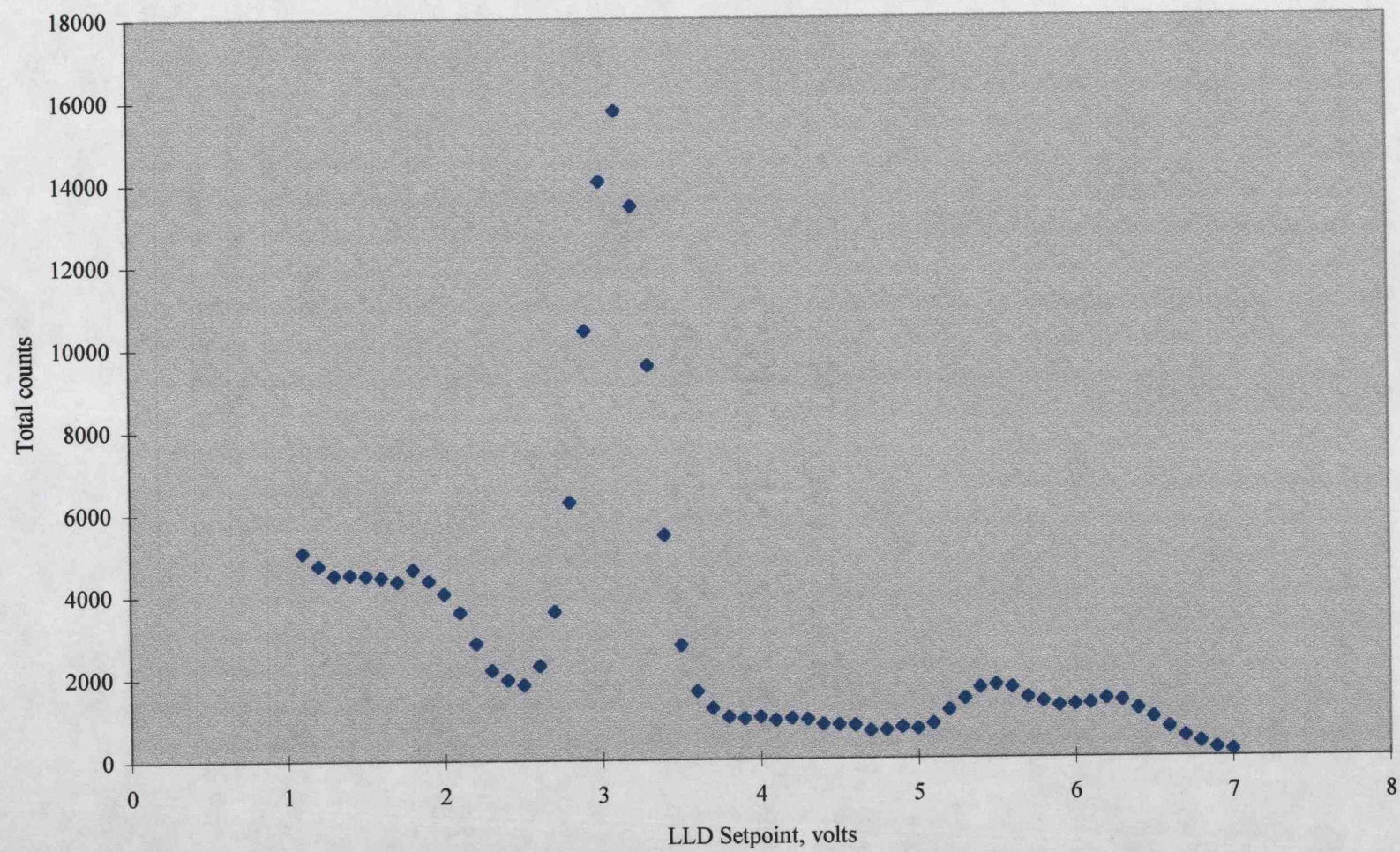


Figure 7. Detector calibration plot - total counts vs. LLD setpoint.

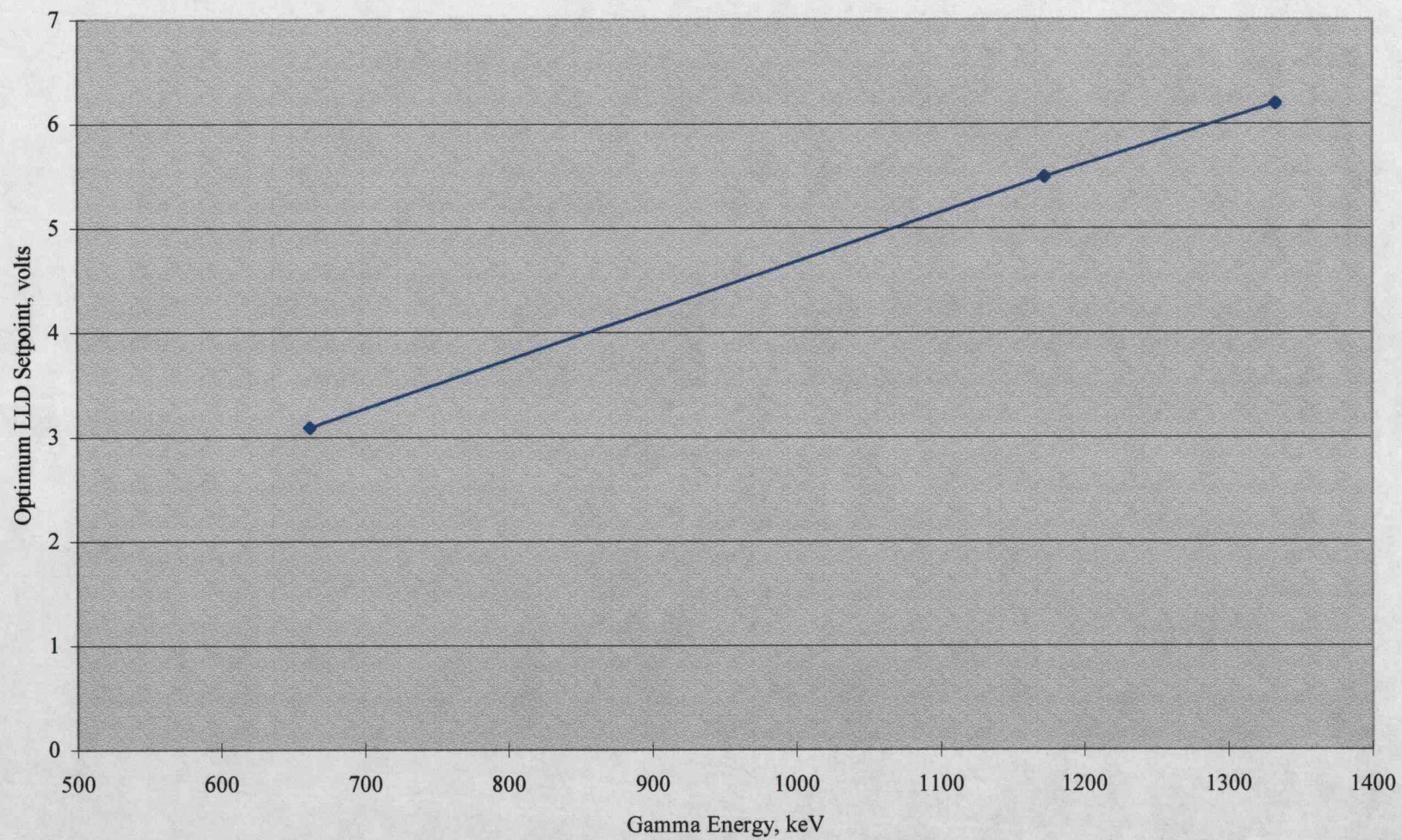


Figure 8. Optimum LLD setting vs. gamma energy plot

where, 'C' is the measured count rate (cps), 'A' is the sample activity (Bq or dps), and Ω is the solid angle. The solid angle is a variable parameter that treats the sample as a point source and accounts for the distance of the source from the detector. Because three different sized containers were used in this experiment, three separate solid angles were calculated. Results are displayed in the Table below. An intrinsic efficiency of 0.0036 was calculated using the counting standard. This intrinsic efficiency as well as the solid angle for a given sample container can then be used to convert measured count rate data to actual sample activity using the equation above.

Solid angle data for sample collection containers.

Sample Type	Diameter of Container (cm)	Solid Angle
sediment, shells	11.43	0.084
water, cockles	8.26	0.133
tissue	5.72	0.200

Marine Ecosystem

Yaquina Bay, in Newport, Oregon, proved a model estuarine ecosystem for this study (Fig. 9). It is one of three Oregon ports dredged to accommodate deep draft vessels as are all of the ports in which U. S. Navy nuclear powered vessels are moored. It is home to a fairly robust marine economy, consisting of both a commercial shellfish and fishing industry as well as heavy recreational and sports fishing use. It is fed with freshwater from the Yaquina River with approximately 1,700 acres of tidewater extending up the bay over an inverted "S" course for 20 km [Marriage, 1958].

In order to model this seasonably cold estuarine environment, a specially designed aquarium system was constructed for the experiment (Figure 10). The main tank was a 50-gallon plastic tub (approximately 107 x 51 x 46 cm). This was housed in a ¾ inch AC plywood box with all void spaces filled with spray foam insulation. The main tank was positioned on a three-foot high plywood stand. The main tank was connected by a vinyl outlet hose to the sump tank, a 30 gallon glass aquarium (76 x 30.5 x 51 cm). The sump tank contained three environmental filters: a particulate bag filter to accept the water output from the main tank and filter gross particulate ($>50\ \mu\text{m}$), a fluidized biological canister filter for harvesting bacteria that convert detritus and other biological waste products to nitrate by nitrification, and a stand alone protein skimmer for oxygen regulation. The sump tank also housed various pumps and plumbing to move water through the filters.

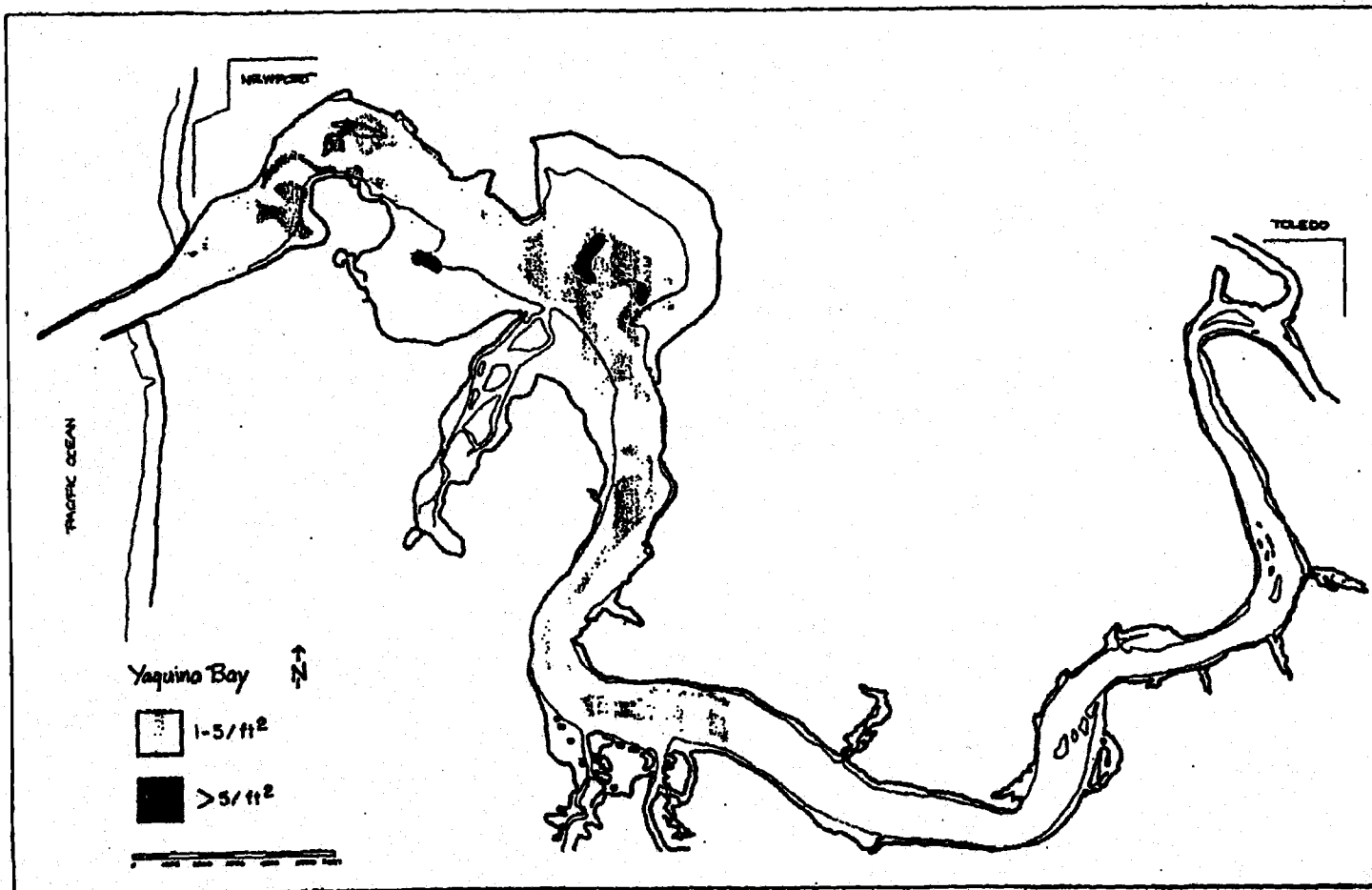
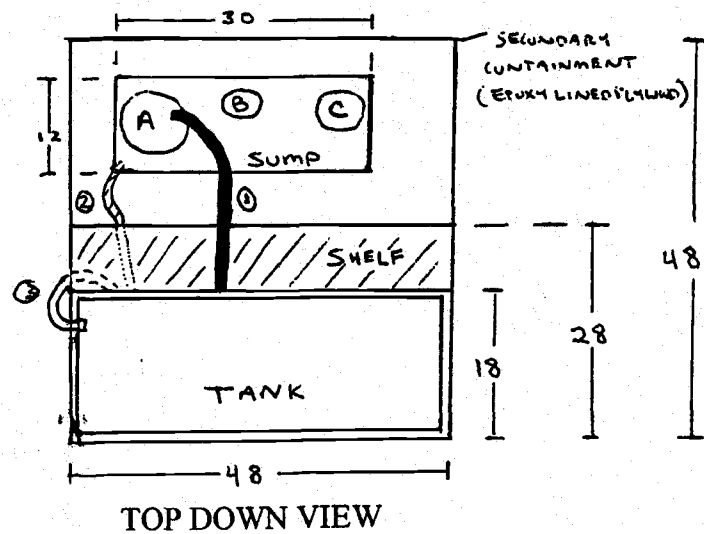


Figure 9. Yaquina Bay, Oregon. From Johnson and Wood (1997)., Copyright © 1997 by Oregon Department of Fish and Wildlife, Salem.
Reprinted by permission of the Oregon Department of Fish and Wildlife.



1. From tank to particulate filter
2. From sump tank to chiller
(chiller located under main tank)
3. From chiller to tank

- A. Particulate (bag) filter
- B. Biological filter
- C. Protein skimmer

REAR VIEW

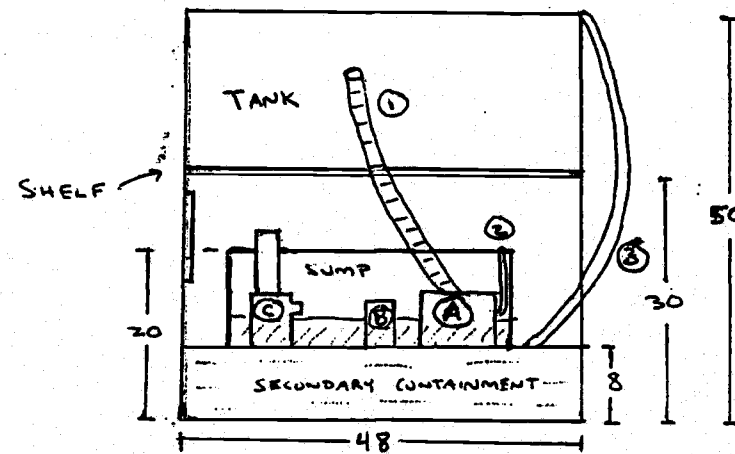


Figure 10. Chilled-seawater aquarium schematic drawing

Water from the sump was then transferred through a 1/5 horsepower chiller back to the main tank.

Sample Collection and Maintenance

The water, sediment, and organisms used in this experiment were all collected at the Oregon State University Hatfield Marine Science Center (HMSC) in Newport, Oregon. Seawater was collected inside the HMSC aquarium wing, from the filtered seawater supply line. This water is drawn directly from Yaquina Bay, filtered to remove oils and chemical impurities, and then used to supply all of the various tanks in the aquarium. Sediment and all benthic organisms were collected from the tidal flats in the bay, directly northeast of the complex (Fig. 11).

The experimental marine ecosystem was first initiated in early January with 150 L of seawater added to the tanks and a 5.0 cm deep sediment layer established along the bottom of the main tank. The chiller was set to maintain a temperature of 51°F, according to reported Yaquina Bay seasonal average water temperature. The system was allowed to recirculate in this mode for several weeks in order to test for proper operation of all of the various subsystems and to culture an adequate bacteria colony for the fluidized bed filter.

Marine organisms were first introduced to the system in late January, following the first of two collection trips to the coast. Several different bivalves and other benthic organisms were collected and observed in the system for suitable radiotracer use, including *Clinocardium nuttallii*, *Mya arenaria* (soft-shell clams),

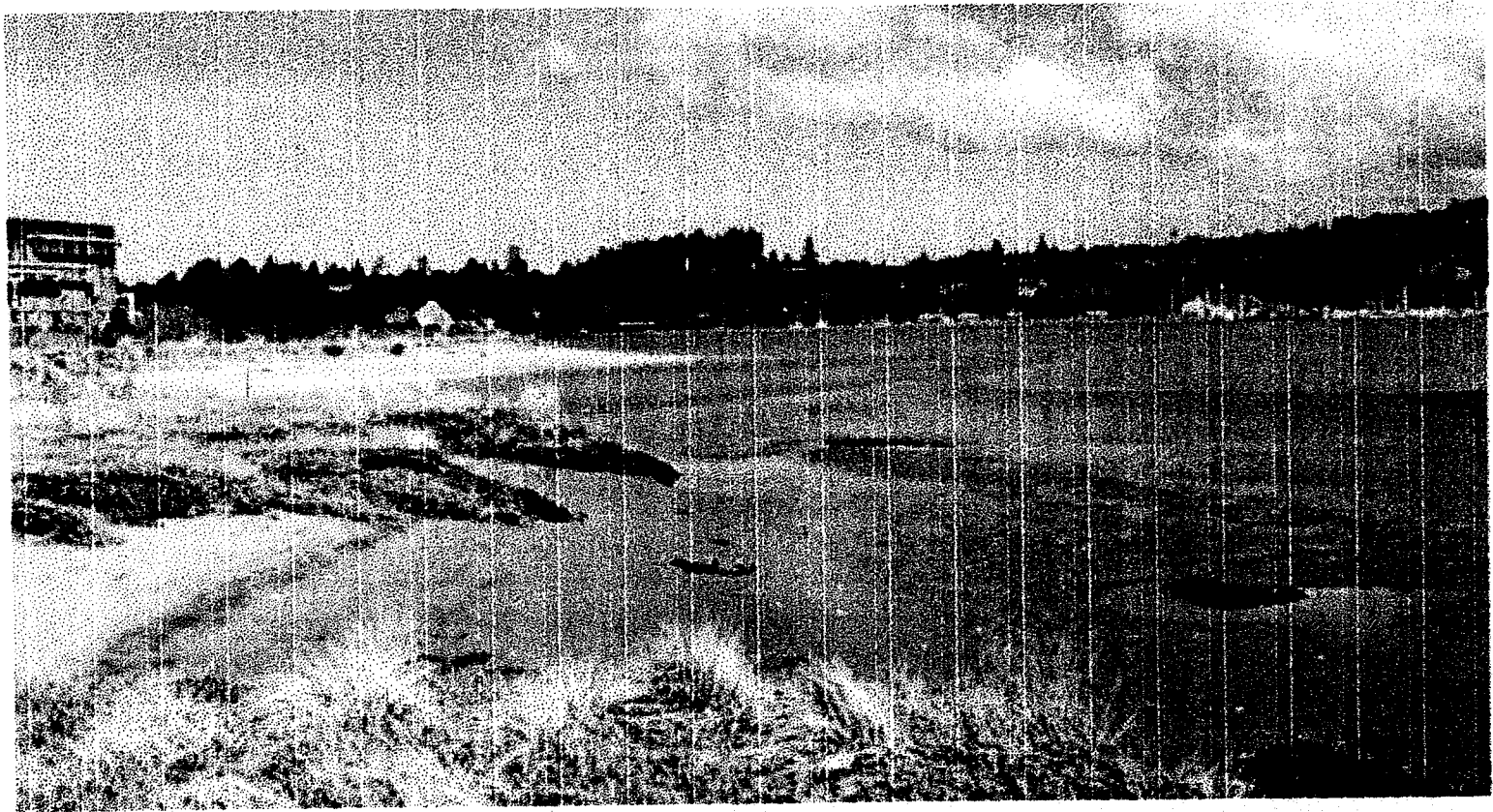


Figure 11. Photograph of Yaquina Bay tidal flats.

Macoma nasuta (bent-nosed clams), ghost shrimp (*Callinassa* sp.), and various lugworms (of undetermined Polychaeta class). The organisms were not fed during this observation period, but routine upkeep of the system was performed. The particulate bag filter was replaced and cleaned biweekly, and the protein skimmer cup was cleaned weekly. Various water changeouts, from 20% to 75% of total system volume were performed as necessary to regulate ammonia and nitrate levels in the system.

Clinocardium nuttallii proved to be the optimum bivalve for this experiment. The soft-shell and bent-nosed clams burrow too deeply for easy collection from the system. The cockle is a shallow burrowing bivalve, residing just below the surface of the sediment, and it was easily located visually by observing extended siphons or strings of fecal matter at the sediment surface or manually by lightly probing the surface with a set of long-handled tongs. The ghost shrimp proved to be too sensitive, breaking apart or being damaged when attempting to remove it from its burrow. The lugworms are useful in removing detritus from the sediment, as is their natural feeding habit, but were far too difficult to locate to be useful for counting.

A second collection trip was undertaken in mid-February. At this time a collection of nine cockles, one bent nose clam (mistaken for a cockle at the time of collection), eight lugworms, and one ghost shrimp (surviving) was gathered and transported one hour back to the laboratory. The cockles represented a wide range

of age and size, from 11.0 g to 108.0 g. The concentration of cockles was limited to avoid gross deviation from observed Yaquina Bay abundance levels of $10.8 / \text{m}^2$ [Johnson and Wood, 1997]. Organisms from the initial collection were removed from the system and discarded along with roughly three-quarters of the sediment and seawater present. Freshly dug sediment and seawater were added to the system along with the newly collected organisms. With all of the elements in place, the system contained 150.0 L of seawater occupying the main tank, sump tank, and associated plumbing. A 10-12 cm deep layer of sediment was spread across the bottom of the main tank.

The organisms were allowed to acclimate to the laboratory setting, and the system was operated under routine upkeep until introduction of the radionuclide in late March. The organisms were fed semi-weekly with a specially designed commercial bivalve nutrient feed, called Roti-Rich™. The powdered supplement, provided by the HMSC staff, was mixed with one liter of distilled water and mixed in a blender at high speed for two minutes. Approximately 100.0 ml of feeding solution was delivered to the main tank and stirred into the water at each feeding. System recirculation was secured during the feedings for 1-3 hours, which resulted in elevated water temperatures reaching as high as 56°F. Intertidal organisms are often exposed to and can withstand varying temperature gradients as can be experienced between tidal periods in their natural habitat, and no deleterious effects were noted. Elevated ammonia levels after feeding evolutions were compensated for by increasing the frequency and volume of seawater changeouts. There was no

means of determining how much of the food was consumed by organisms, but with no deaths observed among cockles maintained in the system throughout the duration of the experiment, it is assumed that they were adequately nourished.

Laboratory Experiment

The remaining 24.0 ml of tracer solution was added to the surface of the main tank at 11:52 AM on 23 March 1999. Using the radioactive decay equation, $A=A_0e^{-\lambda t}$, and a decay time of 8.84 days (time prior to posted activity assay), calculated activity for the ^{59}Fe added to the tank was 1.102 mCi. This gave an initial equilibrium activity concentration of 0.013 $\mu\text{Ci/ml}$ in the main tank, assuming complete mixing with the water volume in the tank. System recirculation was secured for 8.5 hours to allow for natural settling of the radionuclide in the environment and to prevent excessive loss of iron in the system filters. Following restoration of recirculation and adequate mixing time, homogeneous activity concentration would be 0.007 $\mu\text{Ci/ml}$.

During this period sediment, cockle, and several different types of water samples were assayed. Sampling commenced approximately one hour after ^{59}Fe introduction to the aquarium. The system was monitored continuously, with regular sampling, for three weeks, or roughly one half of one half-life for ^{59}Fe .

Seawater from four distinct sources was sampled and assayed for gross activity. Surface and deep water samples were drawn from the main tank using a 5

ml pipette. Each sample was consistently drawn from the same depth within the tank by using the gradation marks on the vertically suspended pipette. Surface samples were drawn from a depth of 4.0 cm and deep samples were drawn from a depth of 18.5 cm. Height above the sediment surface for the deep water samples could not be adequately determined visually and mechanically due to slight sediment height variations across the surface area of the tank. Water from the sump tank particulate filter was also sampled using the 5 ml pipette from the bottom of the filter bag. Water drained from the sediment samples was funneled into a 25 ml flask and assayed as an estimate of interstitial water activity.

Sediment samples were drawn from the upper layer of the sediment using a large plastic serving spoon. The spoon was drawn superficially across the surface of the sediment to minimize disturbance in the ecosystem. The gathered sediment was filtered using medium porosity, medium flow, qualitative filter paper with 8.0 μm particle retention, through a 100 mm diameter funnel. Sediment was allowed to dry for approximately twenty minutes, or until no water drops could be observed following agitation of the funnel. Several of these drained sediment samples were placed in a ventilated hood for 15-22 hours to dry. The sediment samples were subsequently reweighed and the results show an average ratio of dry weight to filtered weight of 0.811. Availability of sample containers precluded complete drying of all sediment samples, and this ratio may prove useful in future experiments when comparing data.

The cockles were withdrawn from the sediment in the bottom of the tank using a pair of long-handled tongs and assayed directly in dry containers. Intertidal organisms are able to withstand prolonged periods of exposure out of water as is natural within their habitat. They use their adductor muscles to tightly close the valves of their shell, retaining water within to meet metabolic needs. Cockles were withdrawn from the system at 1, 8, and 18 days after the ^{59}Fe introduction and frozen for future dissection and internal organ assay. One cockle was removed from the main tank on the tenth day after ^{59}Fe introduction and placed in a "clean" system. This clean system consisted of an 8.0 cm freshly gathered sediment layer and 1.0 L of fresh seawater. This system contained no circulatory system or chilling device and was designed to track iron retention in *Clinocardium nuttallii*.

A tissue distribution study was conducted on the four cockles removed from the system during the experiment. The frozen samples were thawed thirty-two days after the start of the experiment. The liquid was drained from the inside of each cockle, weighed, and counted. The cockles' adductor muscles were severed allowing access to the inside of their shells. The bodies were removed from the shell, and the valves of the shell were weighed and counted. The cockles were then dissected into three distinct masses: the muscular foot, the visceral mass, and the gills and other flesh (including siphons, mantle, and pericardial cavity). Each mass was separately weighed and counted.

All samples were placed in plastic containers for counting to minimize the risk of inadvertent surface contamination. Counting time was initially established

as 100 seconds for all samples. Because of consistently low count rates for the water samples and smaller cockles after one week, the counting time was increased to 400 seconds for these samples. Background count rate was determined before and after each sampling period to determine an average background count rate. Additionally, sample containers were counted at the beginning of each sampling day to check for residual activity that might affect the sample count rate. Based on these results, it was determined that the containers did not significantly absorb the isotope and could be reused. All sample containers and collection instruments were rinsed with either distilled water or clean seawater following each sample. All count rate data collected were background corrected to obtain net count rate data. All data was additionally decay corrected back to the day of radionuclide introduction.

RESULTS

The behavior and movement of ^{59}Fe through an experimental marine ecosystem was closely observed for a period of twenty-two days. This was accomplished under acute, laboratory conditions. Iron was added to the system at the beginning of the experiment and activity levels were monitored in the water, sediment, and the bivalve, *Clinocardium nuttallii*. No additional radionuclide was added to the system during the experiment.

Sediment

Surface sediment samples were collected and counted within two hours of radionuclide introduction to the system. More than one hundred sediment samples ranging in filtered weight from 38.3g to 136.4g (average sample weight was 83.4g) were collected during the experiment. Original data is reported in the Appendix.

The specific count rate (cpm/g) was calculated for each sample. These values are plotted on a linear plot as count rate vs. time after spike (Fig. 12). Mean daily specific count rate (cpm/g) was calculated as the average for all sediment samples taken during a given sampling period and plotted on a linear plot as count rate vs. time after spike (Fig. 13).

During the first day of sampling, very little iron was found in the sediment samples. On the second day of sampling, count rates for sediment samples rapidly increased and remained elevated throughout the experiment. After the initial spike

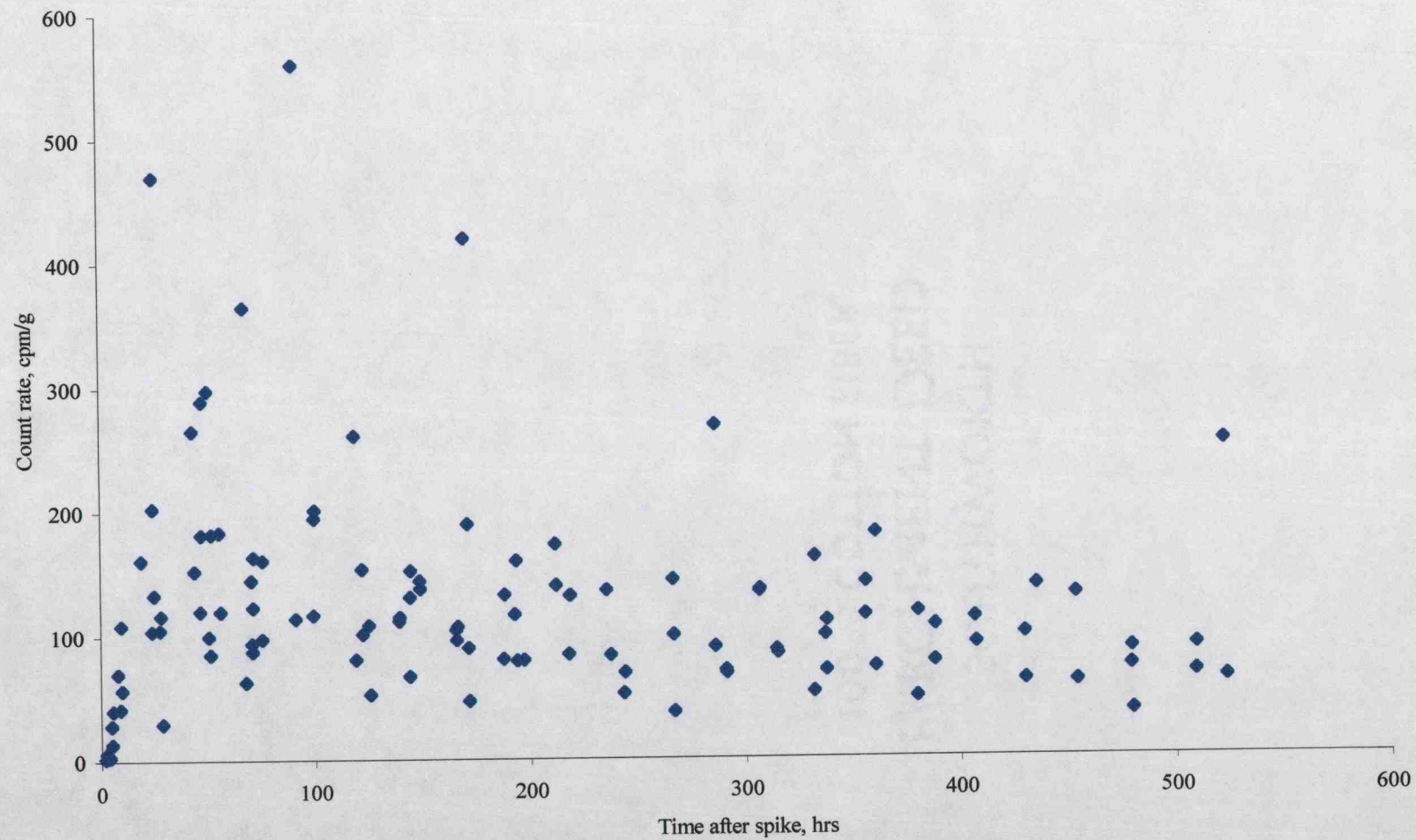


Figure 12. Sediment - specific count rate plot (activity decay corrected)

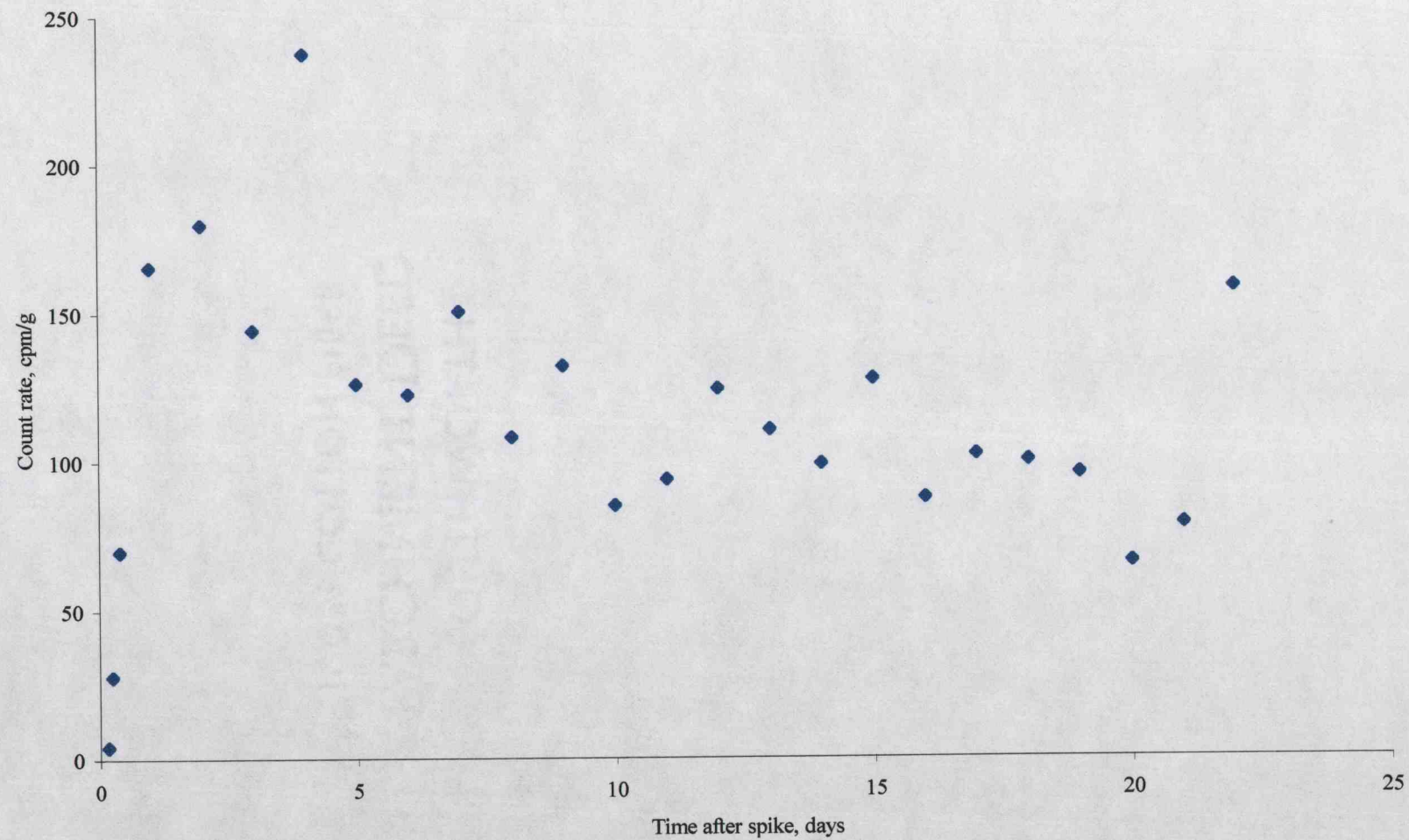


Figure 13. Sediment - mean daily specific count rate plot (activity decay corrected)

in sediment activity, the count rate fell slowly but steadily. A linear regression of the mean daily sediment data after Day 1 shows a weak linear relationship between count rate and time ($R^2 = 0.385$). The slope of the regression line is approximately 4 cpm/g per day.

Water

Water samples from the main tank and bottom (sediment filtered) were collected and counted within two hours of radionuclide introduction. Five hours into the experiment, a decision was made to distinguish between surface and deep water samples within the main tank. This was done in order to investigate possible vertical profiling of ^{59}Fe in the water column. Original data for these three water samples are reported in the Appendix.

The specific count rate (cpm/g) for each water sample and the mean specific count rate (cpm/g) for each daily sampling period were calculated. Some of the water samples registered gross count rates below background count rates. These negative net count rate values were counted as zero for mean specific count rate calculations. Data was plotted as a linear plot of count rate vs. time after spike, and all three sample types were plotted together on the same plot (Figs. 14, 15).

Immediately after ^{59}Fe introduction and the commencement of sampling, there was a rapid increase in main tank water sample count rates. The count rate began to decrease shortly after restoring system recirculation. It decreased steadily until, by the third day of the experiment, gross water sample count rates were

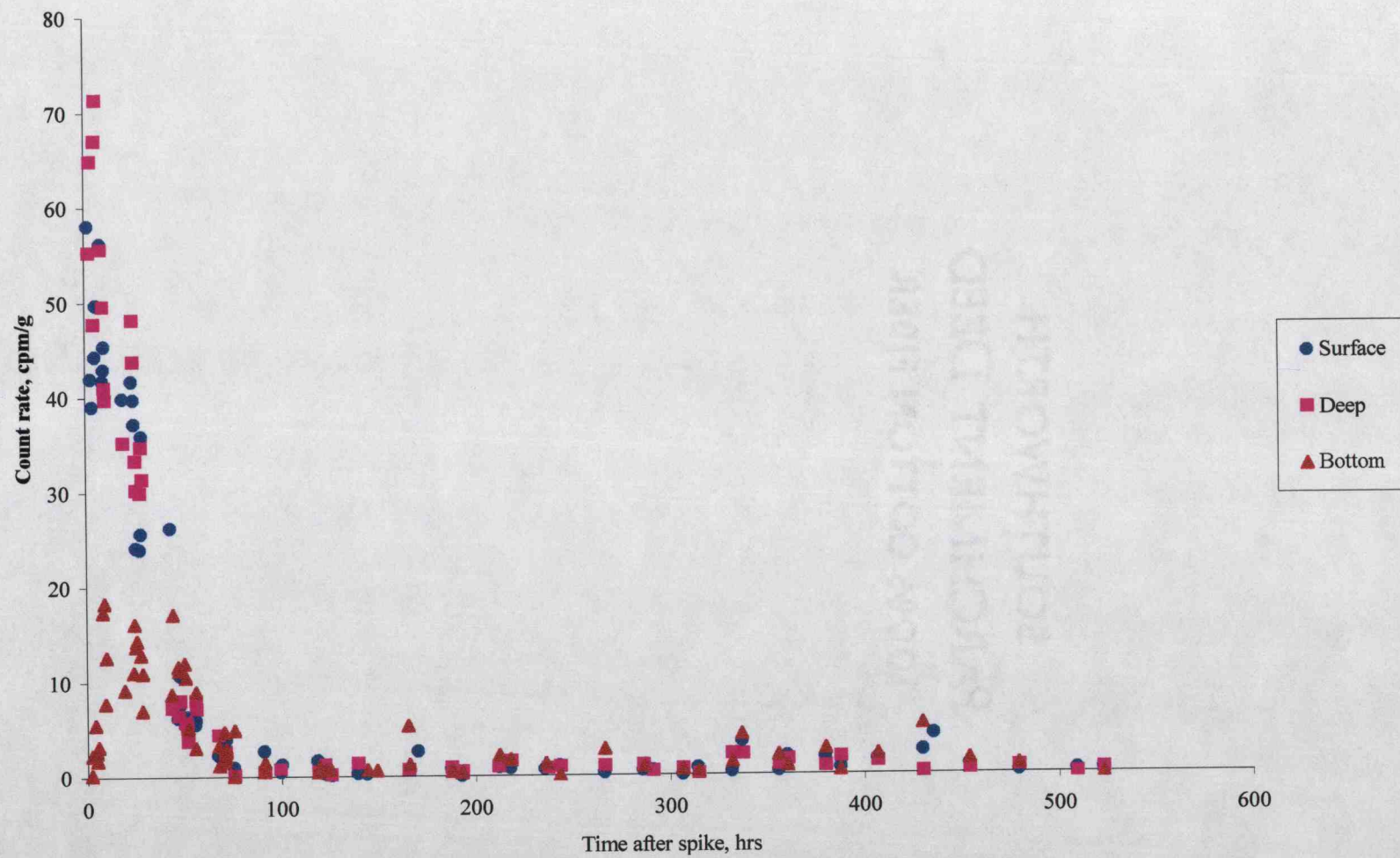


Figure 14. Water - specific count rate plot (activity decay corrected)

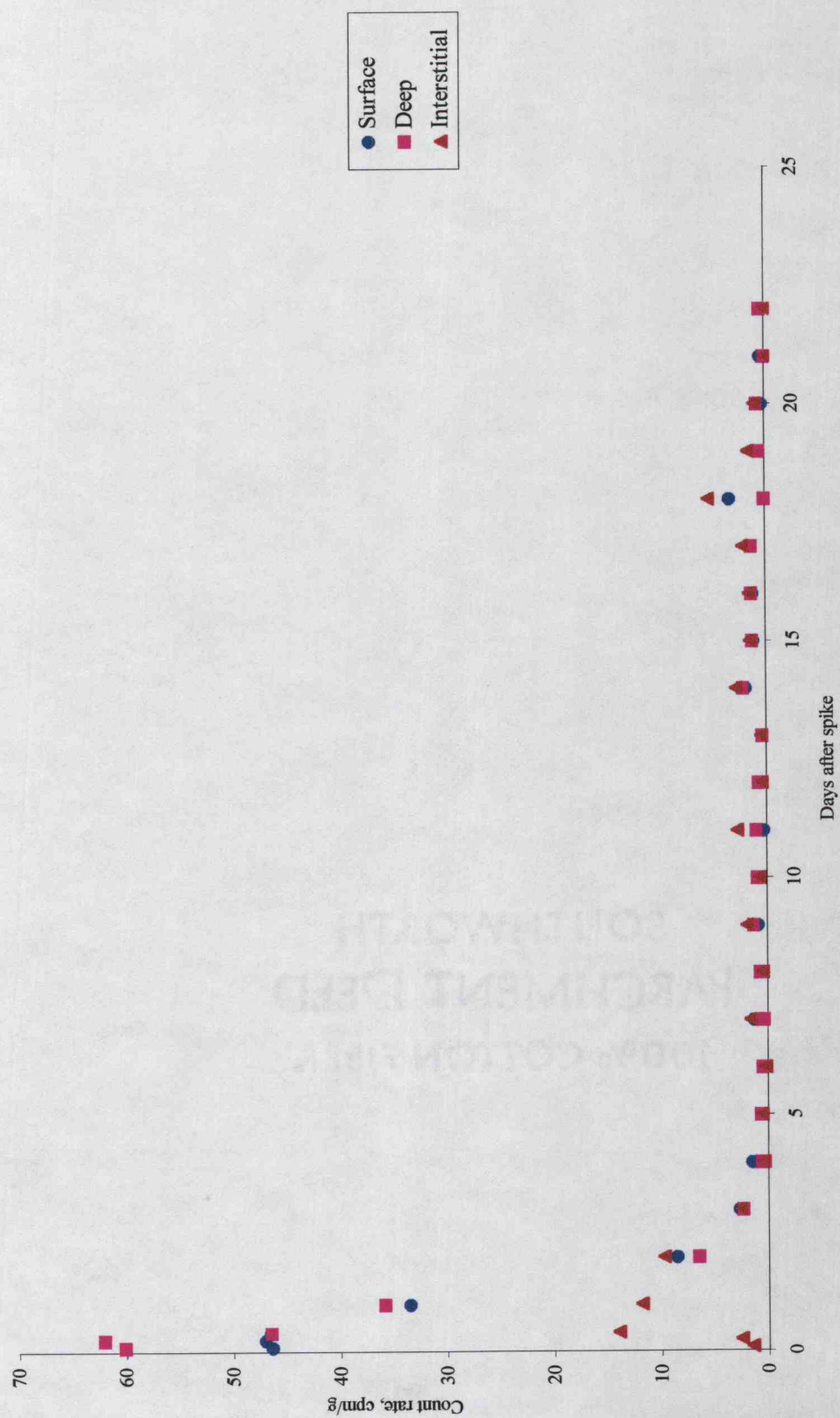


Figure 15. Water - mean daily specific count rate plot (activity decay corrected)

barely higher than background count rates. A linear regression of the mean daily water data for the first three days of the experiment reveals a strong linear relationship between count rate and time for both surface ($R^2 = 0.958$) and deep ($R^2 = 0.926$) water samples. The slopes of the regression lines are approximately 17 cpm/g per day for the surface samples and 22 cpm/g per day for deep samples.

Once system recirculation was restored ten hours into the experiment, periodic water samples were drawn from the sump tank. Initial samples were drawn from various locations within the sump tank. Once it was discovered that count rates were rising in the area of the particulate bag filter relative to samples drawn from outside the filter, all subsequent sump tank water samples were drawn from within the filter.

The specific count rate (cpm/g) was calculated for each sump tank water sample. This data was plotted on a linear plot as count rate vs. time after spike (Figure 16). Ten days after the start of the experiment, the particulate bag filter was removed from the sump tank and replaced with a clean filter. This resulted in a significant change in measured water sample count rates in the sump tank. Before and after filter change out readings were plotted as distinct series to distinguish the two data sets. Original data for the sump tank water samples are reported in the Appendix.

In general, count rates from within the sump tank filter, showed a slight increase over time. Data from sump tank samples taken prior to the changeout of the particulate bag filter did not produce immediately recognizable trends in count

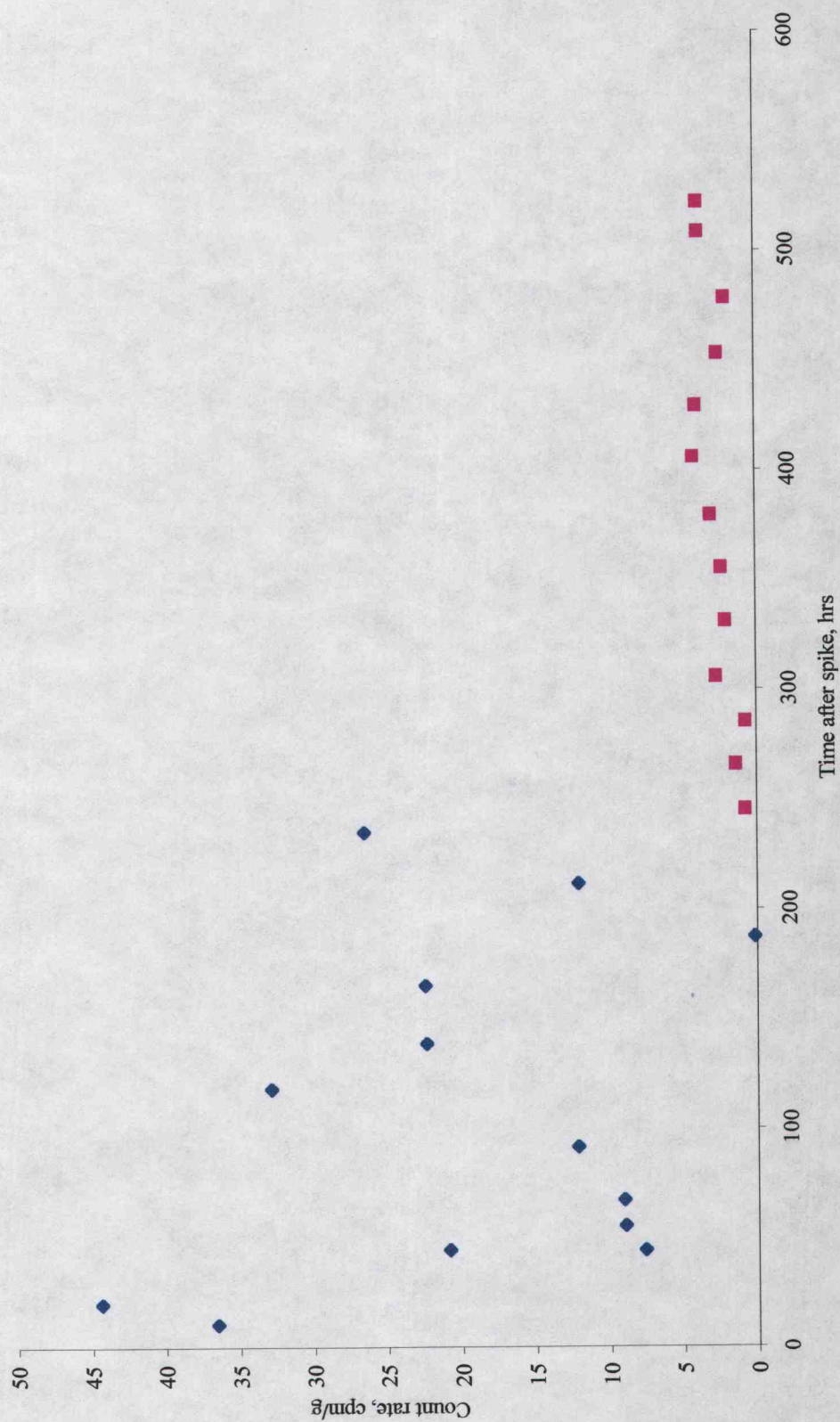


Figure 16. Sump tank water - specific count rate plot (activity decay corrected)

rate. A linear regression of data taken from samples after the changeout, however, does show a linear relationship between count rate and time ($R^2 = 0.542$). The slope of the regression line is approximately 0.24 cpm/g per day.

Bivalves

Cockles were pulled from the system and counted at various times during the experiment. Over the course of the experiment, four of the cockles were permanently removed from the system and frozen for future tissue distribution studies. The remaining cockles were monitored for the duration of the experiment. Original data is reported in the Appendix.

The specific count rate (cpm/g) was calculated for each cockle as it was removed from the system and counted. The cockles, ranging in weight from 11.0g to 108.0g, were each tracked separately, and the results were plotted on a linear plot as count rate vs. time after spike. Because specific count rate for the various cockles tracked very closely, three separate plots were created grouping cockles of similar weight (Figs. 17, 18, and 19). The mean daily specific count rate for all cockles sampled in a given sampling period was then calculated and plotted on a linear plot as count rate vs. time after spike (Fig. 20).

After a rapid uptake during initial exposure to ^{59}Fe in the system, the whole-body count rate for the cockles declined steadily for the remainder of the experiment. A power regression of the mean daily cockle data over the course of



Figure 17. Cockles - specific count rate plot 1 (activity decay corrected)

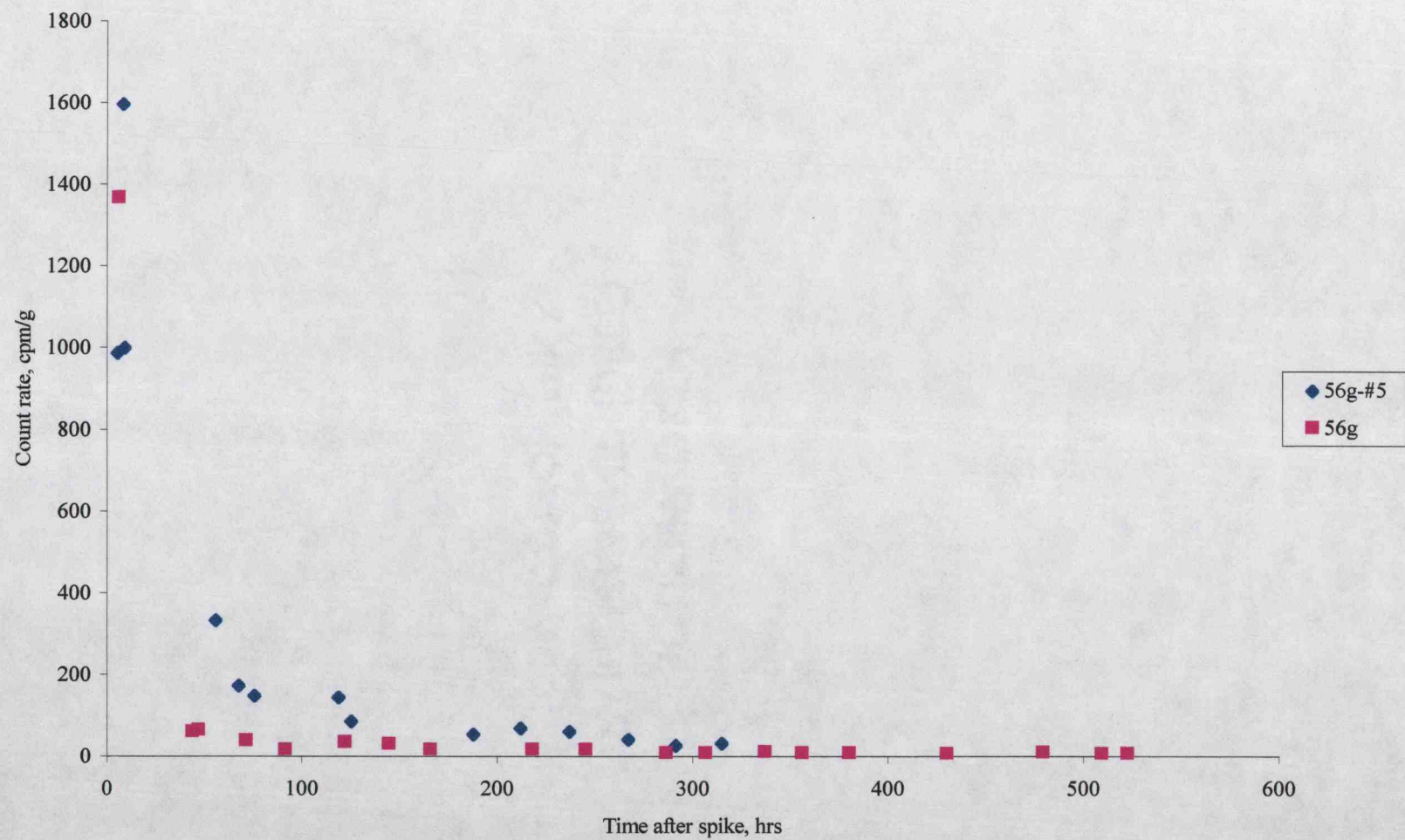


Figure 18. Cockles - specific count rate plot 2 (activity decay corrected)

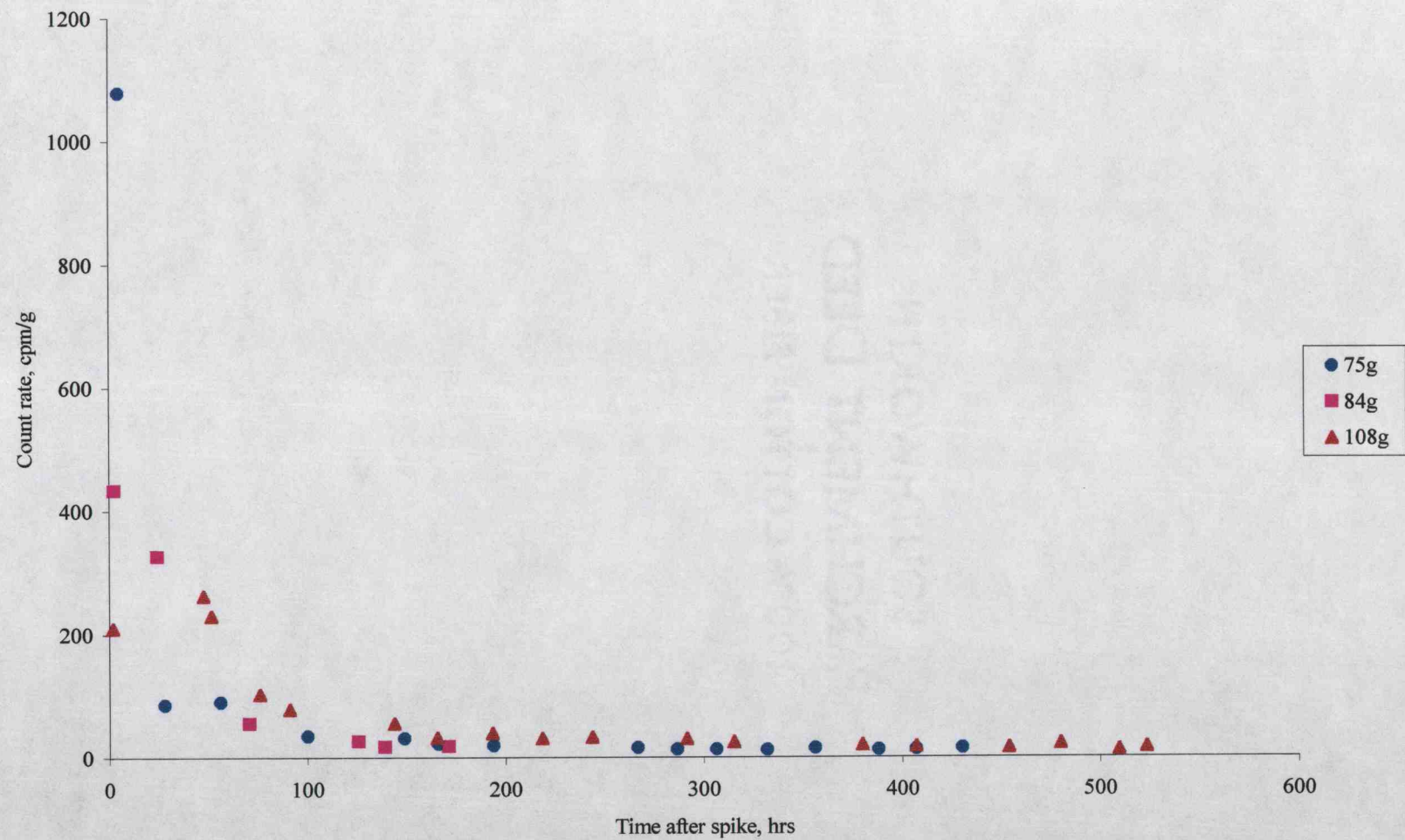


Figure 19. Cockles - specific count rate plot 3 (activity decay corrected)

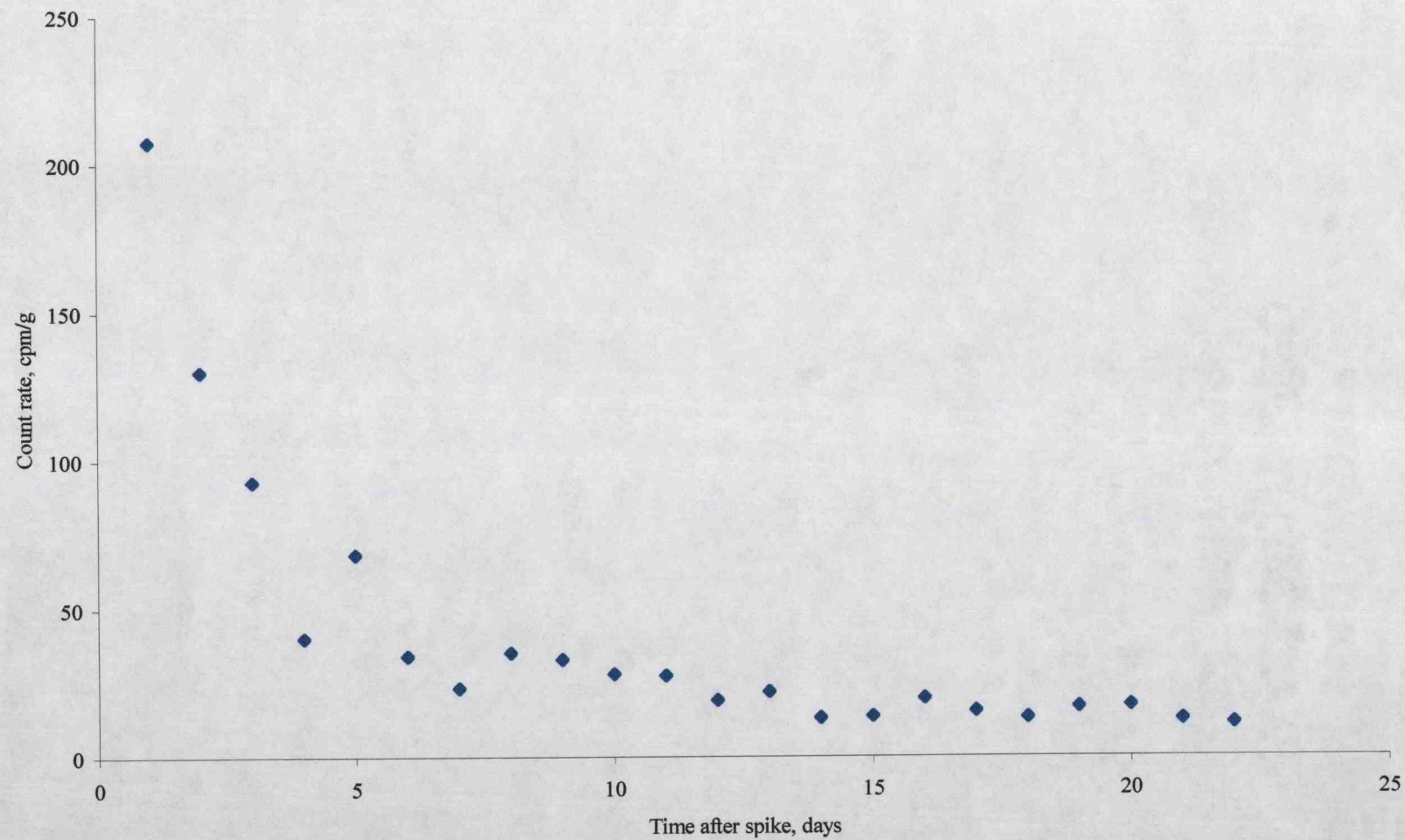


Figure 20. Cockles - mean daily specific count rate plot (activity decay corrected)

the experiment shows a strong correlation between count rate and time ($R^2 = 0.927$). The slope of the regression is approximated by the equation:

$$y = 214.87x^{-0.9255}$$

where 'x' equals the time after spike in days and 'y' equals the specific count rate in cpm/g.

One cockle was removed from the marine system and placed in a container with fresh seawater and non-radioactive sediment on the tenth day of the experiment. This was undertaken in an effort to ascertain ^{59}Fe retention by *Clinocardium nuttallii*. This system had no attached chiller to maintain seasonal temperatures and no external circulatory system. These factors together most likely resulted in the toxic conditions created in this microsystem. The cockle, water, and sediment were sampled and counted over a two-day period. At this point it was obvious that the cockle was deceased. The cockle was removed from the system and frozen for future tissue distribution study. No statistically significant data was produced from this experiment. Original data is reported in the Appendix.

To make a comparison between different bivalve species, the one bent-nose clam, *Macoma nasuta*, was periodically withdrawn from the system and counted. *Macoma nasuta* is a deeper dwelling bivalve that uses a longer siphon to reach the surface of the sediment to feed on suspended organic matter. This particular organism is more selective than *Clinocardium nuttallii* and did not appear to feed as actively. As such, this organism did not appear to accumulate significant ^{59}Fe . The specific count rate (cpm/g) was calculated during each sampling period.

Similar and unremarkable count rates were recorded throughout the experiment.

Original data is reported in the Appendix.

Tissue Distribution Study

The four cockles that were removed during the experiment were thawed and dissected. Five distinct samples were counted from each cockle: pallial fluid (fluid collected and retained within the cockle valves), valves, muscular foot, visceral mass, and gills and other flesh material. Specific count rate (cpm/g) was calculated for each sample, and the values for all components were plotted together on a linear plot as count rate vs. time in system (Fig. 21). Original data is reported in the Appendix.

The specific count rate for each of the cockle tissue components sampled decreased linearly with time. A linear regression of the data shows a firm relationship between count rate and time. R^2 values ranged from 0.64 to 0.89. The slopes of the regression lines ranged from a high of approximately 13 cpm/g per day for the visceral mass to a low of approximately 5 cpm/g per day for the muscular foot. The visceral mass measured the highest specific count rate, with lower measured count rates in the gills and muscular foot respectively. The shell and pallial fluid both measured negligible net count rates, with total count rates approximately equal to background.

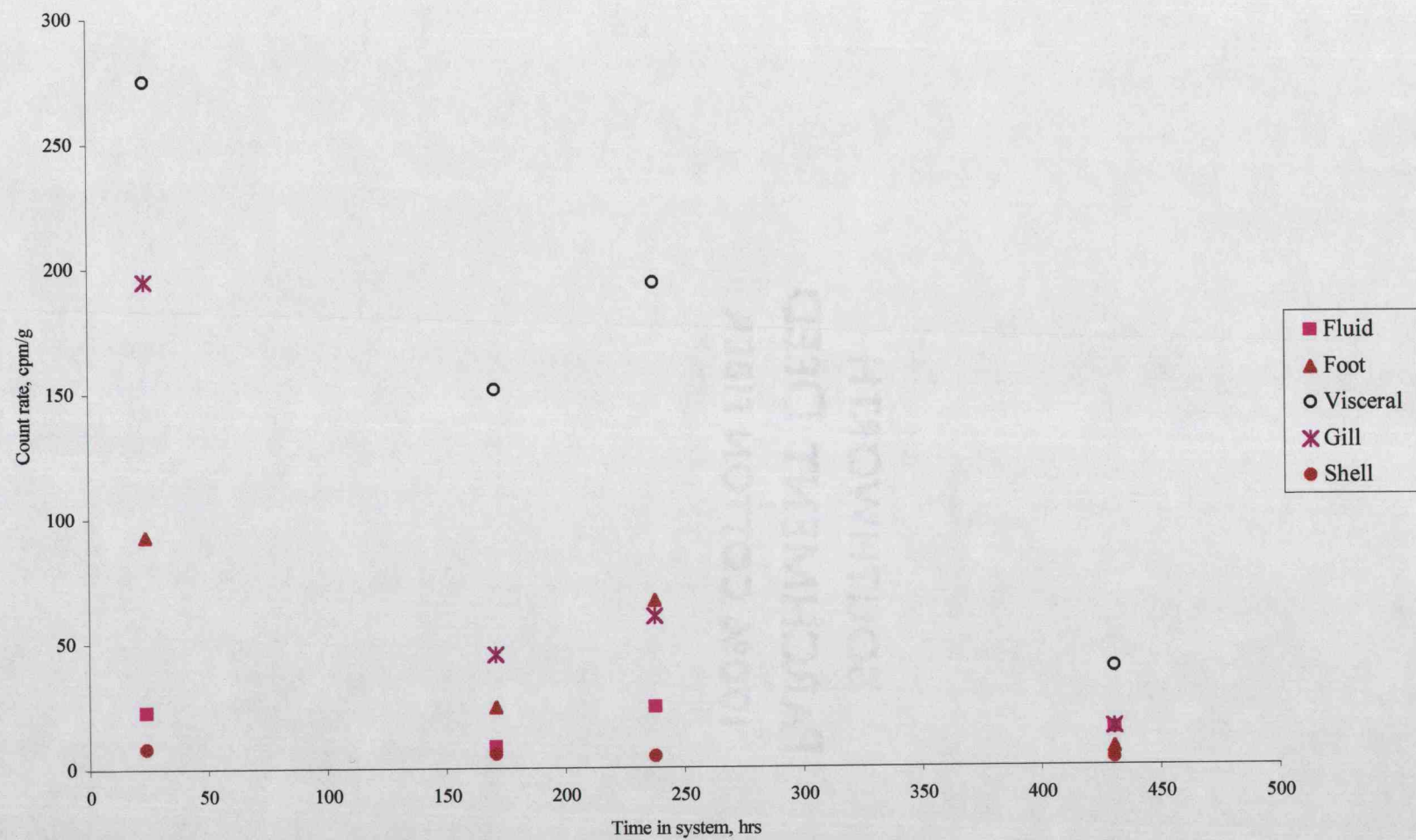


Figure 21. Tissue distribution - specific count rate plot (activity decay corrected)

Error for all data points was calculated as one standard deviation (σ_u) using the formula from Knoll (1989):

$$\sigma_u = (x + y)^{1/2},$$

where 'x' equals total measured counts and 'y' equals measured background counts. This one standard deviation error was applied to all plotted data.

DISCUSSION

The data collected in this experiment provides only a limited model for iron circulation in the marine estuarine environment. Modeling an estuarine ecosystem through a laboratory experiment is an extremely arduous task. A natural estuary is a site of dynamic and rapidly diverging environmental parameters. Temperature and salinity profiles in most areas within this environment change on an hourly basis and undergo a complete cycle twice daily. Without constant supervision or sophisticated computer equipment, these rapid changes cannot be effectively modeled inside a recirculating seawater system.

There, too, are obvious limitations to an in situ ^{59}Fe circulation study. There is an overabundance of variables to account for, uncertainty in tidal patterns, and the need to overcome excessive dilution of the radiotracer. These few examples, along with the relatively short half-life of ^{59}Fe , led to the development of this laboratory experiment. This method of research is in accordance with International Atomic Energy Agency established guidelines for radioecology studies in the marine environment [Chesselet, 1970; Shimizu, 1975], and was undertaken in an effort to capture a microcosm, a snapshot if you will, of this complex meeting of ocean and land.

Iron Speciation

Observations of the behavior of ^{59}Fe after being added to the marine system, support previous research conducted in this area [Pentreath, 1973; Kester *et al.*, 1975; Coughtrey and Thorne, 1983]. These studies showed that most FeCl_3 added to seawater becomes insoluble, adhering to sediments or becoming bound to suspended sediments in the water column. With recirculation secured for the first eight hours of the experiment, the iron was able to react with system constituents much as it would in the natural environment.

Elevated count rates were observed in the unfiltered water samples for the first day of sampling, but then fell off rapidly. By the end of the third day of the experiment, count rates in these unfiltered samples fell off dramatically. Gross counts remained just slightly greater than background counts for the duration of the experiment. This data suggests that iron was being removed from the water column fairly rapidly as suspended particulate matter was grazed by system organisms and lost through filtration. Filtered water sample count rates, support this behavioral pattern of the ^{59}Fe in the system. Water collected from the sediment filters (bottom water) registered negligible net count rates during the first few hours of the experiment, but quickly rose to a peak value. The measured count rates for filtered water samples over the next twenty-four hours were routinely less than 50% that of deep water samples taken at the same time. Purely soluble FeCl_3 should pass through the filter unhindered. This data suggests that much of the iron was insoluble, associated with suspended particulate captured by the filter.

Bottom water count rates fell in unison with the decline in unfiltered water sample count rates, and by the third day of the experiment measured net count rates were similarly insignificant. The low initial count rate does not necessarily indicate a low level of soluble iron in the water column. It likely reflects the observed increase in suspension feeding by *Clinocardium nuttallii* at the start of the experiment. The high feeding capacity of the cockles could easily account for reduced activity levels at the sediment surface. This is supported by high measured count rates for cockles sampled early in the experiment.

One objective of this experiment was to examine the seawater-sediment interface and determine to what degree radioactive iron moves between the two. One parameter used to describe seawater-sediment transfer rates is the sediment:water transfer ratio. Transfer ratio values for radioisotopes of iron in situ are on the order of $\sim 10^6$, and experimental values are in the range $\sim 10^3$ - 10^4 [Coughtrey and Thorne, 1983; Allison *et al.*, 1998]. This ratio is taken as a measure of dry weight sediment concentration ($\mu\text{g Fe/g sediment}$) divided by water concentrations ($\mu\text{g Fe/L seawater}$). A similar parameter is the distribution coefficient (K_D), which is a ratio of the sediment radioactivity (Bq/g) over the water radioactivity (Bq/ml). Recorded values for K_D for ^{59}Fe are 4×10^3 [Koyanagi, 1980] and 5×10^3 [IAEA, 1985].

Data concerning exchange between the sediment and seawater during the experiment is inconclusive. Coughtrey and Thorne (1983) indicate that during leaching experiments nearly 90% of ^{59}Fe that becomes bound to sediment is

unextractable even in highly acidic conditions. This is supported by Koyanagi (1980), who examined the leaching rate of several radioisotopes in seawater of different pH values. At the natural pH of seawater (8.2 by his account), only 1.2% of sediment bound ^{59}Fe leached into the surrounding seawater. Even in an acidic pH of 3.0, only 2.2% of the ^{59}Fe was extracted, suggesting that even the acidic gastric juices in the cockles digestive system would be unable to extract significant iron once bound to the sediment. While pH data was not monitored in this experiment, the frequent seawater changeouts just prior to the experiment as well as the recirculation and filtering of the system's seawater suggest that pH was not nearly acidic enough, even in the bottom sediments, to cause significant leaching.

Because of activity sinks in the system, it is difficult to establish a specific value for the distribution coefficient using the data collected in this study. It does not appear that the system had reached equilibrium with respect to the sediment-seawater interface by the end of the experiment. Even by the twenty-second day of the experiment, decay corrected, mean specific sediment count rates continued to fall at a rate of approximately 10 cpm/g per day while mean specific water activity remained fairly constant. Because there was no observed increase in count rate for any of the other system constituents and because of the observed increase in sump tank filter count rates, it is believed that observed decline in sediment activity could be accounted for by losses through sampling and through system filtration. Correcting the sediment data for these losses yields an approximate K_D of 5×10^2 , which is within an order of magnitude of the previously established values.

Uptake and Retention by *Clinocardium nuttallii*

The *Clinocardium nuttallii* proved to be well suited organisms for this laboratory experiment. All cockles that were maintained in the aquarium survived for the duration of the study and continued to thrive even after data taking was completed. Many of the cockles were quite active during the experiment. Their motion could be traced by tracks left in the sediment and several of the cockles traversed the width of the main tank in less than a day. Consistently during the experiment, cockles employed their natural escape mechanisms, using their strong, muscular feet to rapidly move laterally when contacted by the sampling tongs. They fed actively throughout the study, often maintaining open siphons for extended periods while organic matter concentrations were low. The siphons quickly closed in a defensive response to shadows or surface disturbances. The cockles exhibited a large feeding capacity, quickly grazing down food stocks and producing copious feces and pseudofeces strings during feeding periods. The cockles appear to have exhibited behavioral patterns closely mirroring those in their natural estuarine environment.

The results of the experiment indicate that the primary means of ^{59}Fe uptake for *Clinocardium nuttallii* is through the filter-feeding process. Uptake of ^{59}Fe was very rapid in the early stages of the experiment. Visual observations confirm that the cockles were actively filtering water during radionuclide introduction. Suspended particulate, on which the iron had sorbed, would be drawn in through the incurrent siphon and captured in the cockle's gill filaments. With elevated

measured activity levels in the water column for the first 48-72 hours of the experiment, the cockles would have processed contaminated organic matter in the water column as well as residual soluble iron in the filtered water during this period.

While no data was available with regard to the duration of digestive cycle of *Clinocardium nuttallii*, other studies with suspension feeding bivalves indicate that pseudofeces generation will occur quite rapidly after feeding, within the first several hours. Digested material, feces, will then normally be observed approximately 6-10 hours after feeding [Bayne, 1993; Jørgensen, 1996; Allison *et al.*, 1998]. Visual observations of the system confirm this pattern, as increased generation of feces and pseudofeces was observed during the second day of sampling following radionuclide introduction. This pattern continued for several days.

This effect may have been exacerbated by the experimental methods employed in this study. Securing the chiller and recirculation to add the iron to the system may have triggered a feeding response in the organisms. Consistently during the period leading up to introduction of ^{59}Fe to the system, cockles were observed with siphons fully extended shortly after securing recirculation for feeding or seawater changeouts. The cockles likely adapted to their environment to anticipate a period of high organic content in the water column.

CONCLUSION

Summary

This experiment successfully confirms that the previously established pattern for iron speciation in the open ocean can be extended to the intertidal and estuarine environments. When radioactive iron was introduced to the experimental marine system, it rapidly adhered to suspended particulate within the water column. It was then transported to the sediment layer at the bottom of the system as the particulate was allowed to settle. In its travels from the near surface to the sediment layer it was subject to a variety of physical, biological, and chemical forces. Among these were internal water circulation, changing salinity and pH conditions, and biological consumption by filter feeding organisms. Despite these external forces, the majority of radionuclide remained bound to the particulate and became a semi-permanent component of the sediment layer. This experiment provided insufficient evidence to support substantive transfer of bound ^{59}Fe from the sediment to the cockles that filtered sediment while feeding.

In the natural environment, ^{59}Fe introduced into the estuarine environment would be subject to significantly varied physical, biological, and chemical forces as compared to those observed in this experiment. Tidal and current flow would disperse suspended particulate with bound ^{59}Fe over a much wider area. Large salinity variations within an open estuarine system occur vertically as well as horizontally. Numerous suspended and freely swimming organisms would graze

suspended particulate from the water column before reaching the sediment interface where benthic organisms such as *Clinocardium nuttallii* feed.

Still, the data collected in this experiment provides an excellent basis to begin to assess the impact of a maritime radiological accident. Discharge of reactor effluent water by a moored nuclear powered submarine or surface ship would release significant levels of ^{59}Fe into the local estuarine environment. This experiment has shown that the majority of iron would be sorbed onto particulate matter and deposited over an area in the direct vicinity of the ship. Any radiobiological impact would then be limited to organisms residing in this finite area. *Clinocardium nuttallii* and other similarly sessile, filter-feeding organisms can provide critical data concerning the potential environmental impact of such a release as they consume suspended particulate and process contaminated sediment.

Recommendation for Future Research

This experiment did not provide sufficient independent data to accurately assess the rate of uptake and retention of ^{59}Fe by *Clinocardium nuttallii*. Future experiments would need to control the level of ^{59}Fe in the system, such that the cockles consume identifiable levels of contaminated particulate and that their fecal matter and discharged fluids can be collected and analyzed for iron retention. Many similar experiments have been undertaken using other benthic organisms, such as *Mytilus edulis*, and are widely accepted by the scientific community. This

data would be valuable when trying to assess the radiobiological impact of ^{59}Fe in seawater on this species of cockle.

A more extensive tissue study is necessary to accurately assess tissue distribution of ^{59}Fe in *Clinocardium nuttallii*. Such an experiment should include a larger pool of cockles to improve the accuracy of the data. Tissue distribution studies conducted on other similar species have shown a tendency to concentrate radionuclides in the gills when attached to inorganic particles and in the stomach or visceral mass when bound to organic matter. An extensive tissue distribution study would help determine whether ^{59}Fe more readily associates with organic or inorganic matter and whether or not it is more readily extracted by the organism in either form. This data could then be used to determine biological impacts on a contaminated population based on feeding patterns as well as turbulence at the seawater-sediment interface.

Future studies are also needed to assess the true radiobiological impact of a maritime nuclear accident. Iron-59 is just one constituent of reactor effluent water. Many other radionuclides would be released to the marine environment. Some, such as ^{60}Co and ^{137}Cs , have been well studied and have relatively long half-lives. These radionuclides behave far differently from ^{59}Fe in the marine environment with different residence times and widely varying radiobiological impacts. To make an accurate assessment of the effect of such a release on the estuarine environment, future research is necessary in order to understand the behavior in the marine environment of each radionuclide constituent of reactor effluent water.

BIBLIOGRAPHY

- Allison, N., Millward, G. E. and Jones, M. B. 1998. Particle processing by *Mytilus edulis*: effects on the bioavailability of metals. *Journal of Experimental Marine Biology and Ecology*, 222:149-162
- Aston, S. R. 1978. Estuarine chemistry. In *Chemical oceanography* (J. P. Riley and R. Chester, eds.). Vol. 7. 2d. ed. New York: Academic Press.
- Barnes, R. D. 1980. *Invertebrate zoology*. 4th ed. Philadelphia: Saunders College.
- Bayne, B. L. 1993. Feeding physiology of bivalves: time dependence and compensation for changes in food availability. In *Bivalve filter feeders in estuarine and coastal ecosystem processes* (R. Dame, ed.). New York: Springer-Verlag.
- Burton, J. D. 1975. Radioactive nuclides in the marine environment. In *Chemical oceanography* (J. P. Riley and G. Skirrow, eds.). Vol. 3. 2d. ed. New York: Academic Press.
- Carpenter, R. and Peterson, M. L. 1989. Chemical cycling in Washington's coastal zone. In *Coastal oceanography of Washington and Oregon* (M. R. Landry and B. M. Hickey, eds.). *Elsevier Oceanography Series* 47. Amsterdam: Elsevier.
- Chesselet, E. 1970. Review of the techniques of measuring stable and radioactive Ru, Mn, Cr, Fe and Zr-Ni in a marine environment. In *Reference methods for marine radioactivity studies*. *IAEA Technical Report Series No. 118*. Vienna: International Atomic Energy Agency.
- Coimbra, J. and Carraça, S. 1990. Accumulation of Fe, Zn, Cu, and Cd during the different stages of the reproductive cycle in *Mytilus edulis*. *Comparative Biochemistry and Physiology*, 95c(2):265-270.
- Coughtrey, P. J. and Thorne, M. C. 1983. *Radionuclide distribution and transportation in terrestrial and aquatic ecosystems*. Vol. 2. Rotterdam: A. A. Balkema.
- Dahlgaard, H. 1994. Marine radioecology. In *Radioecology: lectures in environmental radioactivity* (E. Holm, ed.). Lund, Sweden: World Scientific.

- DOD/DOE. 1998. The United States Naval Nuclear Propulsion Program. Pub no. 1998-609-000-80011. Bethesda: U. S. Government Printing Office.
- Duursma, E. K. 1976. Radioactive tracers in estuarine chemical studies. In *Estuarine chemistry* (J. D. Burton and P. S. Liss, eds.). London: Academic Press.
- Eisenbud, M. and Gesell, T. 1997. *Environmental radioactivity from natural, industrial, and military sources*. 4th ed. San Diego: Academic Press.
- Evan, S. 1984. Uptake and loss of ^{134}Cs and ^{60}Co by the Baltic bivalve *Macoma baltica* in a laboratory microcosmos. *Journal of Environmental Radioactivity*, 1:133-150.
- Hamilton, T. F., Fowler, S. W., Larosa, J., Holm, E., Smith, J. D., Aarkrog, A., and Dahlgaard, H. 1991. Comparative study of plutonium and americium bioaccumulation from two marine sediments contaminated in the natural environment. *Journal of Environmental Radioactivity*, 14:211-223.
- Hancock, D. R., Gauner, T. F., Willeke, G. B., Robart, G. P., and Flynn, J. 1979. *Subtidal clam populations: distribution, abundance and ecology*. Pub no. ORESU-T-79-002. Newport: Oregon State University Sea Grant College Program.
- IAEA, 1985. Sediment K_D 's and concentration factors for radionuclides in the marine environment. *IAEA Technical Report Series No. 247*. Vienna: International Atomic Energy Agency
- Johnson, J. A. and Wood, C. 1997. *1996 Oregon bay clam data series report*. Newport, Oregon: Oregon Department of Fish and Wildlife.
- Jørgensen, C. B. 1990. *Bivalve filter feeding: hydrodynamics, bioenergetics, physiology and ecology*. Denmark: Olsen & Olsen.
- Jørgensen, C. B. 1996. Bivalve filter feeding revisited. *Marine Ecology Progress Series* 142:287-302.
- Kester, D. R., Byrne, Jr., R. H., and Liang, Y. 1975. Redox reactions and solution complexes of iron in marine systems. In *Marine chemistry in the coastal environment* (T. M. Church, ed.). *ACS Symposium Series 18*. Washington, D. C.: American Chemical Society.
- Knoll, G. F. 1989. *Radiation detection and measurement*. 2d. ed. New York: John Wiley & Sons, Inc.

- Koyanagi, T. 1980. Effect of sediment-bound radionuclides on marine organisms. *In* Radiation effects on aquatic organisms (N. Egami, ed.). Baltimore: University Park Press.
- Kozloff, E. N. 1987. *Marine invertebrates of the Pacific Northwest*. Seattle: University of Washington Press.
- Marriage, L. D. 1958. Bay clams of Oregon. *Educational Bulletin No. 2*. Salem: Fish Commission of Oregon.
- McDonald, P., Baxter, M. S., and Fowler, S. W. 1993a. Distribution of radionuclides in mussels, winkles and prawns. part 1. Study of organisms under environmental conditions using conventional radio-analytical techniques. *Journal of Environmental Radioactivity*, 18:181-202.
- McDonald, P., Baxter, M. S., and Fowler, S. W. 1993b. Distribution of radionuclides in mussels, winkles and prawns. part 2. Study of organisms under environmental conditions using conventional radio-analytical techniques. *Journal of Environmental Radioactivity*, 18:203-228.
- Navarro, E., and Iglesias, J. 1992. Infaunal filter-feeding bivalves and the physiological response to short-term fluctuations in food availability and composition. *In* *Bivalve filter feeders in estuarine and coastal ecosystem processes* (R. Dame, ed.). New York: Springer-Verlag.
- NAS 1971. *Radioactivity in the marine environment*. Washington, D. C.: National Academy Press
- Newell, R. C. 1979. *Biology of intertidal animals*. 3d. ed. Faversham: Marine Ecological Surveys Ltd.
- Paakkola, O. 1994. Sample collection and processing. *In* *Radioecology: lectures in environmental radioactivity* (E. Holm, ed.). Lund, Sweden: World Scientific.
- Pechenik, J. A. 1996. *Biology of the invertebrates*. 3d. ed. Dubuque: Wm. C. Brown Publishers.
- Pentreath, R. J. 1973. The accumulation from water of Zn-65, Mn-54, Co-58 and Fe-59 by the mussel *Mytilus edulis*. *Journal of the Marine Biological Association of the U. K.*, 53:127-143

- Price, N. B. 1976. Chemical diagenesis in sediments. In *Chemical Oceanography* (J. P. Riley and R. Chester, eds.). Vol. 6. 2d ed. New York: Academic Press.
- Ratti, F. D. 1978. Reproduction and growth of the Pacific basket-cockle, *Clinocardium nuttallii* Conrad, from intertidal and subtidal environments of Netarts Bay. M. S. thesis. Corvallis: Oregon State University
- Ricketts, E. F., Calvin, J., and Hedgepeth, J. W. 1985. *Between Pacific tides*. 5th ed. Stanford: Stanford University Press.
- Schleien, B. (ed.) 1992. *The health physics and radiological health handbook*. Silver Springs, Maryland: Scinta, Inc.
- Shimizu, M. 1975. Procedures for radioecological studies with molluscs. In Design of radiotracer experiments in marine biological systems. *IAEA Technical Report Series No. 167*. Vienna: International Atomic Energy Agency.
- Wallace, R. L., Taylor, W. K., Litton, Jr., J. R. 1989. Beck and Braithwaite's *Invertebrate zoology: a laboratory manual*. 4th ed. New York: MacMillan Publishing.
- Young, D. R., and Folsom, T. R. 1972. Mussels and barnacles as indicators of the variation of ⁵⁴Mn, ⁶⁰Co and ⁶⁵Zn in the marine environment (IAEA-SM-158/42). In *Radioactive contamination of the marine environment*. Vienna: International Atomic Energy Agency.

APPENDIX

Appendix Table 1. Sediment sample count rate data.

Cs+b	Cb	Count time, sec	Net wt., g(l)	Count rate cpm/g	Time after spike, hrs.	Gross count rate, cpm	Decay corrected count rate, cpm/g
675	305	100	86.6	2.564	2.13	222.0	2.567
1121	305	100	74.1	6.607	2.70	489.6	6.619
1020	305	100	88.7	4.837	3.17	429.0	4.846
825	305	100	88.2	3.537	4.28	312.0	3.547
2160	305	100	38.3	29.060	4.90	1113.0	29.153
1651	305	100	56.7	14.243	5.28	807.6	14.292
3180	305	100	42.5	40.588	5.75	1725.0	40.740
5312	323	100	42.7	70.103	8.30	2993.4	70.482
3496	323	100	45.1	42.213	9.13	1903.8	42.464
8940	323	100	47.7	108.390	9.68	5170.2	109.073
7094	323	100	71.1	57.139	10.10	4062.6	57.515
11887	319	100	43.5	159.559	19.37	6940.8	161.577
8173	347	100	45.5	103.200	24.13	4695.6	104.829
19695	347	100	58.0	200.152	24.68	11608.8	203.384
19095	347	100	85.6	131.411	25.27	11248.8	133.584
47622	347	100	61.4	461.971	25.80	28365.0	469.771
7961	375	100	44.0	103.445	27.88	4551.6	105.334
14489	375	100	73.9	114.593	28.37	8468.4	116.722
3609	375	100	65.6	29.579	28.93	1940.4	30.140
25451	468	100	58.0	258.445	43.60	14989.8	265.863
16584	468	100	65.2	148.307	44.37	9669.6	152.640
11487	426	100	56.7	117.048	47.02	6636.6	120.675
24700	426	100	82.5	176.538	47.45	14564.4	182.059
27031	426	100	56.9	280.545	48.00	15963.0	289.422
27036	365	100	55.5	288.335	50.55	16002.6	297.952
15261	365	100	92.1	97.042	50.92	8937.6	100.303
10150	365	100	71.1	82.574	51.67	5871.0	85.390
16980	365	100	56.6	176.131	52.12	9969.0	182.191
16360	393	100	54.1	177.083	55.85	9580.2	183.620
11804	393	100	59.2	115.652	56.30	6846.6	119.956
44098	416	100	75.1	348.991	67.65	26209.2	364.655
8511	416	100	80.3	60.486	68.02	4857.0	63.216
19896	376	100	84.5	138.604	70.68	11712.0	145.110
12702	376	100	82.4	89.752	71.02	7395.6	93.986
11441	376	100	79.4	83.615	71.27	6639.0	87.573
10320	376	100	50.7	117.680	71.50	5966.4	123.270
24616	376	100	93.1	156.219	71.73	14544.0	163.664
14318	351	100	90.2	92.907	75.72	8380.2	97.587
25812	351	100	99.7	153.226	76.05	15276.6	160.978
17841	373	100	97.4	107.606	91.15	10480.8	114.164
79371	373	100	89.8	527.826	91.43	47398.8	560.095
12209	337	100	65.0	109.588	99.38	7123.2	116.889
30669	337	100	99.8	182.357	99.83	18199.2	194.563
21381	337	100	66.8	189.018	100.23	12626.4	201.722

Appendix Table 1 (Continued). Sediment sample count rate data.

Cs+b	Cb	Count time, sec	Net wt., g(1)	Count rate cpm/g	Time after spike, hrs.	Gross count rate, cpm	Decay corrected count rate, cpm/g
32802	336	100	80.6	241.682	118.77	19479.6	261.049
13519	336	100	105.4	75.046	119.13	7909.8	81.078
21673	344	100	90.2	141.878	122.12	12797.4	153.581
17140	344	100	107.8	93.484	122.43	10077.6	101.215
13655	364	100	79.7	100.058	125.30	7974.6	108.535
6727	364	100	78.5	48.634	125.65	3817.8	52.767
16751	373	100	96.3	102.044	139.20	9826.8	111.692
17309	373	100	96.8	104.975	139.50	10161.6	114.923
7793	403	100	72.4	61.243	143.93	4434.0	67.240
17504	403	100	86.0	119.309	144.26	10260.6	131.019
19772	403	100	83.7	138.846	144.57	11621.4	152.504
19743	406	100	88.6	130.950	148.62	11602.2	144.211
23631	406	100	111.3	125.202	148.95	13935.0	137.910
9986	411	100	61.1	94.026	165.52	5745.0	104.689
9724	411	100	64.5	86.633	165.88	5587.8	96.480
12795	411	100	77.1	96.374	166.22	7430.4	107.352
38323	374	100	60.6	375.733	170.57	22769.4	419.717
22431	374	100	78.0	169.669	171.02	13234.2	189.586
14920	374	100	108.1	80.736	171.37	8727.6	90.234
4842	374	100	63.1	42.485	171.67	2680.8	47.492
13364	316	100	109.1	71.758	187.67	7828.8	81.053
21004	316	100	105.5	117.657	188.10	12412.8	132.934
18121	308	100	103.8	102.965	193.05	10687.8	116.709
16436	308	100	68.5	141.267	193.68	9676.8	160.189
8664	308	100	71.5	70.120	194.10	5013.6	79.534
13086	317	100	109.0	70.288	197.12	7661.4	79.881
29727	281	100	117.1	150.876	212.02	17667.6	173.134
18781	281	100	90.8	122.247	212.28	11100.0	140.304
16959	296	100	136.1	73.459	217.90	9997.8	84.618
15735	296	100	80.9	114.504	218.60	9263.4	131.958
21337	296	100	110.4	114.353	218.85	12624.6	131.806
26449	337	100	134.4	116.571	235.78	15667.2	135.847
12821	218	100	105.4	71.744	237.47	7561.8	83.699
8295	223	100	107.9	44.886	243.50	4843.2	52.571
7961	223	100	78.4	59.219	244.02	4642.8	69.382
22596	221	100	110.6	121.383	266.42	13425.0	144.296
12117	221	100	85.0	83.972	266.73	7137.6	99.842
5356	221	100	97.6	31.568	267.02	3081.0	37.541
14283	271	100	112.4	74.797	286.13	8407.2	90.061
32338	271	100	86.4	222.688	286.63	19240.2	268.217
9342	310	100	92.1	58.840	291.10	5419.2	71.076
9097	310	100	92.7	56.874	291.42	5272.2	68.715
18836	266	100	100.8	110.536	306.60	11142.0	134.872
16735	223	100	88.8	111.568	306.88	9907.2	136.156

Appendix Table 1 (Continued). Sediment sample count rate data.

Cs+b	Cb	Count time, sec	Net wt., g(l)	Count rate cpm/g	Time after spike, hrs.	Gross count rate, cpm	Decay corrected count rate, cpm/g
13949	221	100	115.9	71.068	314.53	8236.8	87.162
11305	221	100	96.5	68.916	315.13	6650.4	84.556
6842	223	100	92.6	42.888	331.97	3971.4	53.199
25882	223	100	117.9	130.580	332.3	15395.4	162.009
11841	215	100	87.5	79.721	337.27	6975.6	99.229
7116	215	100	73.1	56.643	337.62	4140.6	70.519
11461	367	100	74.9	88.870	338.05	6656.4	110.673
16663	201	100	108.3	91.202	355.9	9877.2	114.900
16637	201	100	87.7	112.447	356.25	9861.6	141.697
12100	216	100	123.3	57.830	360.62	7130.4	73.080
23950	216	100	99.4	143.264	360.98	14240.4	181.085
8416	236	100	128.9	38.076	379.95	4908	48.724
16005	236	100	103.0	91.858	380.4	9461.4	117.581
8769	243	100	84.9	60.254	387.92	5115.6	77.505
13673	243	100	97.5	82.646	388.23	8058	106.329
12413	269	100	84.4	86.332	406.82	7286.4	112.419
14402	269	100	120.2	70.547	407.18	8479.8	91.886
9103	312	100	70.0	75.351	429.88	5274.6	99.600
5459	312	100	65.9	46.862	430.32	3088.2	61.960
16104	476	100	89.9	104.303	435.6	9376.8	138.380
13153	192	100	79.8	97.451	453.8	7776.6	130.827
5388	192	100	69.3	44.987	454.1	3117.6	60.406
10094	196	100	110.9	53.551	479.2	5938.8	73.086
7451	196	100	68.0	64.015	479.53	4353	87.386
3243	196	100	67.7	27.004	479.97	1828.2	36.874
9545	219	100	114.8	48.742	509.33	5595.6	67.837
8202	219	100	74.4	64.379	509.68	4789.8	89.620
22486	212	100	74.1	180.356	522.95	13364.4	253.240
5828	212	100	75.0	44.928	523.45	3369.6	63.104

Appendix Table 2. Surface water sample count rate data.

Cs+b	Cb	Count time, sec	Net wt., g	Count rate cpm/g	Time after spike, hrs.	Gross count rate, cpm	Decay corrected count rate, cpm/g
4309	305	100	41.4	58.029	1.72	2402.4	58.094
1997	305	100	24.2	41.950	2.80	1015.2	42.027
2014	305	100	26.3	38.989	3.38	1025.4	39.074
2301	305	100	27.1	44.192	5.12	1197.6	44.339
2353	305	100	24.8	49.548	5.92	1228.8	49.739
2597	323	100	24.4	55.918	8.25	1364.4	56.218
1984	323	100	24.0	41.525	9.08	996.6	41.770
2089	323	100	24.8	42.726	9.53	1059.6	42.991
2097	323	100	23.6	45.102	10.02	1064.4	45.396
1894	319	100	24.0	39.375	19.27	945.0	39.871
2003	347	100	24.2	41.058	24.02	993.6	41.703
1912	347	100	24.0	39.125	24.62	939.0	39.755
1830	347	100	24.3	36.617	25.12	889.8	37.219
1308	347	100	24.3	23.728	25.73	576.6	24.128
1317	375	100	24.0	23.550	27.80	565.2	23.979
1403	375	100	24.5	25.176	28.30	616.8	25.642
1790	375	100	24.1	35.228	28.88	849.0	35.895
1497	468	100	24.2	25.512	43.50	617.4	26.243
789	468	100	24.3	7.926	44.11	192.6	8.156
665	426	100	23.8	6.025	46.96	143.4	6.212
714	426	100	23.7	7.291	47.40	172.8	7.519
841	426	100	24.1	10.332	47.93	249.0	10.658
615	365	100	24.5	6.122	50.43	150.0	6.326
590	365	100	24.3	5.556	50.85	135.0	5.742
616	365	100	24.6	6.122	51.58	150.6	6.330
579	365	100	24.0	5.350	52.08	128.4	5.534
602	393	100	23.4	5.359	55.78	125.4	5.557
621	393	100	23.6	5.797	56.23	136.8	6.012
504	416	100	23.6	2.237	67.57	52.8	2.338
504	376	100	24.1	3.187	70.63	76.8	3.336
488	376	100	23.9	2.812	71.23	67.2	2.945
491	376	100	18.3	3.770	71.67	69.0	3.950
390	351	100	24.1	0.971	75.67	23.4	1.020
475	373	100	23.6	2.593	91.10	61.2	2.751
357	337	100	23.4	0.513	99.48	12.0	0.547
387	337	100	24.9	1.205	100.17	30.0	1.286
399	336	100	23.9	1.582	118.67	37.8	1.708
359	344	100	29.8	0.302	122.08	9.0	0.327
342	364	100	23.7	-0.557	125.23	-13.2	-0.604
410	364	100	178.8	0.154	125.85	27.6	0.167
387	373	100	24.4	0.344	139.15	8.4	0.377
414	403	100	23.5	0.281	143.90	6.6	0.308
391	406	100	24.3	-0.370	148.57	-9.0	-0.408
386	411	100	23.7	-0.633	165.48	-15.0	-0.705

Appendix Table 2 (Continued). Surface water sample count rate data.

Cs+b	Cb	Count time, sec	Net wt., g	Count rate cpm/g	Time after spike, hrs.	Gross count rate, cpm	Decay corrected count rate, cpm/g
1840	1464	400	23.7	2.380	170.40	56.4	2.658
1360	1246	400	22.9	0.747	187.50	17.1	0.843
1316	1307	400	23.2	0.058	192.90	1.4	0.066
1381	1255	400	23.4	0.808	211.92	18.9	0.927
1400	1281	400	24.1	0.741	217.77	17.9	0.853
1391	1293	400	23.1	0.636	235.57	14.7	0.741
1047	907	400	23.4	0.897	243.22	21.0	1.051
978	936	400	23.6	0.267	266.30	6.3	0.317
1121	1047	400	23.9	0.464	286.02	11.1	0.559
1229	1162	400	23.0	0.437	290.85	10.1	0.528
1180	1173	400	22.9	0.046	306.37	1.1	0.056
934	838	400	23.2	0.621	314.25	14.4	0.761
928	880	400	23.8	0.303	331.85	7.2	0.375
1315	862	400	23.9	2.843	337.02	68.0	3.538
883	832	400	23.4	0.327	355.78	7.7	0.412
1088	843	400	23.7	1.551	360.33	36.8	1.959
1092	870	400	23.3	1.429	379.83	33.3	1.829
1059	972	400	24.3	0.537	387.68	13.1	0.691
1214	1021	400	23.7	1.222	406.70	29.0	1.591
1416	1118	400	23.5	1.902	429.77	44.7	2.514
2413	1897	400	24.4	3.172	435.45	77.4	4.208
898	777	400	24.0	0.756	453.68	18.2	1.015
857	822	400	24.6	0.213	479.06	5.3	0.291
885	833	400	24.7	0.316	509.20	7.8	0.439
854	802	400	23.5	0.332	522.83	7.8	0.466

Appendix Table 3. Deep water sample count rate data.

Cs+b	Cb	Count time, sec	Net wt., g	Count rate cpm/g	Time after spike, hrs.	Gross count rate, cpm	Decay corrected count rate, cpm/g
2567	305	100	24.6	55.171	2.46	1357.2	55.259
3133	305	100	26.2	64.763	3.12	1696.8	64.895
2366	305	100	26.0	47.562	4.52	1236.6	47.701
3098	305	100	25.1	66.765	5.62	1675.8	67.009
3255	305	100	24.9	71.084	6.02	1770.0	71.363
2617	323	100	24.9	55.277	8.47	1376.4	55.582
2310	323	100	24.2	49.264	9.32	1192.2	49.563
2008	323	100	24.8	40.766	9.90	1011.0	41.029
1960	323	100	24.9	39.446	10.30	982.2	39.710
1731	319	100	24.4	34.721	19.57	847.2	35.165
2369	347	100	25.6	47.391	24.37	1213.2	48.146
1946	347	100	22.3	43.022	24.90	959.4	43.723
1712	347	100	25.0	32.760	25.57	819.0	33.308
1535	347	100	24.0	29.700	25.97	712.8	30.205
1583	375	100	24.7	29.344	28.07	724.8	29.884
1739	375	100	24.0	34.100	28.57	818.4	34.738
1600	375	100	23.9	30.753	29.12	735.0	31.340
763	468	100	25.2	7.024	43.85	177.0	7.227
676	426	100	24.2	6.198	47.23	150.0	6.391
740	426	100	24.6	7.659	47.70	188.4	7.899
746	426	100	24.7	7.773	48.18	192.0	8.020
591	365	100	24.4	5.557	50.68	135.6	5.743
598	365	100	25.6	5.461	51.13	139.8	5.645
569	365	100	24.8	4.935	51.83	122.4	5.104
514	365	100	24.8	3.605	52.28	89.4	3.729
714	393	100	24.9	7.735	56.08	192.6	8.022
669	393	100	24.2	6.843	56.52	165.6	7.099
602	416	100	26.4	4.227	67.95	111.6	4.418
458	376	100	24.5	2.008	70.93	49.2	2.103
479	376	100	24.8	2.492	71.45	61.8	2.610
359	351	100	24.9	0.193	75.97	4.8	0.203
393	373	100	25.3	0.474	91.37	12.0	0.503
365	337	100	22.5	0.747	99.75	16.8	0.797
360	336	100	25.2	0.571	119.03	14.4	0.617
392	344	100	25.2	1.143	122.35	28.8	1.237
371	364	100	24.2	0.174	125.52	4.2	0.188
423	373	100	24.0	1.250	139.40	30.0	1.368
393	403	100	24.7	-0.243	144.20	-6.0	-0.267
389	406	100	25.9	-0.394	148.88	-10.2	-0.434
1677	1583	400	24.9	0.566	165.73	14.1	0.631
1325	1464	400	25.0	-0.834	170.87	-20.9	-0.932
1377	1246	400	24.8	0.792	187.95	19.7	0.895
1393	1307	400	29.7	0.434	193.47	12.9	0.492
1390	1255	400	24.3	0.833	212.17	20.3	0.956

Appendix Table 3 (Continued). Deep water sample count rate data.

Cs+b	Cb	Count time, sec	Net wt., g	Count rate cpm/g	Time after spike, hrs.	Gross count rate, cpm	Decay corrected count rate, cpm/g
1494	1281	400	24.1	1.326	218.33	32.0	1.528
969	865	400	23.7	0.658	237.33	15.6	0.768
1044	907	400	24.9	0.825	243.82	20.6	0.967
1081	936	400	26.8	0.812	266.60	21.8	0.965
1194	1047	400	24.7	0.893	286.45	22.1	1.075
1216	1162	400	24.1	0.336	291.30	8.1	0.406
920	832	400	24.5	0.539	306.72	13.2	0.657
853	838	400	24.8	0.091	314.97	2.3	0.111
1170	880	400	24.9	1.747	332.18	43.5	2.167
1684	1397	400	24.8	1.736	337.50	43.1	2.161
958	832	400	24.7	0.765	356.10	18.9	0.964
1053	843	400	25.7	1.226	360.80	31.5	1.549
981	870	400	24.9	0.669	380.20	16.7	0.856
1203	972	400	24.7	1.403	388.08	34.7	1.805
1183	1021	400	24.5	0.992	407.02	24.3	1.292
2055	2037	400	23.8	0.113	430.08	2.7	0.150
1672	1897	400	25.2	-1.339	435.75	-33.8	-1.777
838	777	400	24.5	0.373	453.98	9.2	0.501
915	822	400	26.2	0.532	479.42	14.0	0.727
830	833	400	24.6	-0.018	509.53	-0.5	-0.025
862	802	400	30.7	0.293	523.17	9.0	0.412

Appendix Table 4. Bottom (interstitial) water sample count rate data.

Cs+b	Cb	Count time, sec	Net wt., g	Count rate cpm/g	Time after spike, hrs.	Gross count rate, cpm	Decay corrected count rate, cpm/g
308	305	100	7.7	0.234	2.30	1.8	0.234
377	305	100	18.8	2.298	2.70	43.2	2.302
284	305	100	6.3	-2.000	3.22	-12.6	-2.004
388	305	100	9.0	5.533	4.33	49.8	5.549
343	305	100	8.6	2.651	4.95	22.8	2.660
358	305	100	18.1	1.757	5.32	31.8	1.763
360	305	100	10.3	3.204	5.83	33.0	3.216
752	323	100	14.9	17.275	8.37	257.4	17.369
609	323	100	9.4	18.255	9.18	171.6	18.364
569	323	100	19.1	7.728	9.73	147.6	7.777
614	323	100	13.9	12.561	10.23	174.6	12.645
637	319	100	21.0	9.086	19.47	190.8	9.201
673	347	100	18.0	10.867	24.23	195.6	11.039
649	347	100	11.4	15.895	24.75	181.2	16.152
607	347	100	11.5	13.565	25.38	156.0	13.791
721	347	100	15.9	14.113	25.85	224.4	14.352
554	375	100	8.5	12.635	27.92	107.4	12.866
523	375	100	12.9	6.884	28.42	88.8	7.012
616	375	100	13.5	10.711	28.98	144.6	10.914
736	468	100	18.9	8.508	43.68	160.8	8.753
776	468	100	11.1	16.649	44.43	184.8	17.136
759	426	100	17.7	11.288	47.07	199.8	11.638
788	426	100	20.0	10.860	47.52	217.2	11.200
502	365	100	7.1	11.577	50.47	82.2	11.963
595	365	100	13.6	10.147	51.00	138.0	10.489
483	365	100	14.4	4.917	52.18	70.8	5.086
474	393	100	16.4	2.963	55.90	48.6	3.073
471	393	100	5.4	8.667	56.35	46.8	8.989
490	416	100	14.1	3.149	67.72	44.4	3.290
450	416	100	16.9	1.207	68.08	20.4	1.262
462	376	100	11.4	4.526	70.72	51.6	4.739
421	376	100	16.8	1.607	71.07	27.0	1.683
445	376	100	20.7	2.000	71.30	41.4	2.095
424	376	100	11.4	2.526	71.57	28.8	2.646
455	376	100	16.3	2.908	71.77	47.4	3.047
355	351	100	20.5	0.117	75.80	2.4	0.123
419	351	100	8.7	4.690	76.10	40.8	4.927
389	373	100	16.4	0.585	91.22	9.6	0.621
422	373	100	20.7	1.420	91.52	29.4	1.507
325	337	100	17.1	-0.421	99.60	-7.2	-0.449
329	337	100	14.7	-0.327	99.88	-4.8	-0.348
335	337	100	17.6	-0.068	100.28	-1.2	-0.073
352	336	100	20.0	0.480	118.82	9.6	0.518
365	336	100	18.9	0.921	119.20	17.4	0.995

Appendix Table 4 (Continued). Bottom (interstitial) water sample count rate data.

Cs+b	Cb	Count time, sec	Net wt., g	Count rate cpm/g	Time after spike, hrs.	Gross count rate, cpm	Decay corrected count rate, cpm/g
354	344	100	10.3	0.583	122.18	6.0	0.631
362	344	100	16.9	0.639	122.50	10.8	0.692
378	364	100	13.9	0.604	125.37	8.4	0.656
356	364	100	8.0	-0.600	125.68	-4.8	-0.651
338	373	100	8.8	-2.386	139.25	-21.0	-2.612
370	373	100	20.9	-0.086	139.53	-1.8	-0.094
373	403	100	15.4	-1.169	143.98	-18.0	-1.283
422	403	100	18.0	0.633	144.32	11.4	0.696
378	406	100	15.3	-1.098	148.68	-16.8	-1.209
418	406	100	12.7	0.567	149.00	7.2	0.624
475	411	100	8.0	4.800	165.57	38.4	5.345
1686	1583	400	13.8	1.120	166.00	15.5	1.247
1453	1464	400	19.1	-0.086	170.65	-1.7	-0.097
1329	1464	400	21.6	-0.938	171.10	-20.3	-1.048
1289	1246	400	13.1	0.492	187.72	6.5	0.556
1345	1307	400	17.6	0.324	193.08	5.7	0.367
1395	1255	400	11.0	1.909	212.32	21.0	2.191
1452	1281	400	17.0	1.509	217.95	25.7	1.738
1002	865	400	18.7	1.099	236.12	20.6	1.281
910	907	400	12.2	0.037	243.55	0.5	0.043
1142	936	400	13.2	2.341	266.62	30.9	2.783
1117	1047	400	13.5	0.778	286.18	10.5	0.937
1099	1162	400	15.0	-0.630	290.97	-9.5	-0.761
1245	1173	400	22.4	0.482	306.48	10.8	0.588
888	838	400	21.6	0.347	314.60	7.5	0.426
992	880	400	15.2	1.105	332.03	16.8	1.371
1285	862	400	18.6	3.411	337.13	63.5	4.246
959	832	400	11.7	1.628	355.93	19.1	2.051
928	843	400	17.0	0.750	360.47	12.8	0.948
1101	870	400	16.4	2.113	379.98	34.7	2.704
1011	972	400	15.4	0.380	387.80	5.9	0.489
1169	1021	400	13.6	1.632	406.87	22.2	2.126
1608	1118	400	18.2	4.038	429.92	73.5	5.338
902	777	400	15.5	1.210	453.83	18.8	1.624
898	822	400	15.8	0.722	479.23	11.4	0.985
803	833	400	17.6	-0.256	509.37	-4.5	-0.356
803	802	400	17.5	0.009	523.00	0.2	0.012

Appendix Table 5. Sump tank water sample count rate data.

Cs+b	Cb	Count time, sec	Net wt., g	Count rate cpm/g	Time after spike, hrs.	Gross count rate, cpm	Decay corrected count rate, cpm/g
1722	323	100	23.1	36.338	10.43	839.40	36.584
2014	319	100	23.2	43.836	19.92	1017.00	44.407
770	468	100	24.3	7.457	44.30	181.20	7.674
1277	468	100	23.9	20.310	44.53	485.40	20.905
741	393	100	24.0	8.700	55.55	208.80	9.019
763	416	100	23.9	8.711	67.37	208.20	9.101
819	373	100	23.3	11.485	91.63	267.60	12.189
1630	336	100	25.5	30.447	118.28	776.40	32.876
1257	373	100	25.9	20.479	138.95	530.40	22.411
1262	411	100	25.3	20.182	165.32	510.60	22.468
323	316	100	23.7	0.177	187.35	4.20	0.200
3098	1255	400	26.2	10.552	211.63	276.45	12.105
5379	1293	400	26.9	22.784	235.36	612.90	26.545
<hr/>							
1012	907	400	23.8	0.662	245.63	15.75	0.776
1135	936	400	25.3	1.180	266.05	29.85	1.402
1151	1047	400	25.1	0.622	285.78	15.60	0.748
1527	1173	400	24.1	2.203	306.13	53.10	2.688
1150	880	400	24.8	1.633	331.63	40.50	2.025
1126	832	400	24.2	1.822	355.58	44.10	2.295
1278	870	400	26.1	2.345	379.62	61.20	3.000
1551	1021	400	24.8	3.206	406.48	79.50	4.173
1617	1118	400	25.0	2.994	429.57	74.85	3.957
1111	777	400	26.8	1.869	453.47	50.10	2.509
1021	822	400	20.4	1.463	478.88	29.85	1.997
1326	833	400	27.1	2.729	509.00	73.95	3.797
1284	802	400	26.6	2.718	522.63	72.30	3.816

Appendix Table 6. Cockle sample count rate data.

Cs+b	Cb	Count time, sec	Net wt., g(1)	Count rate cpm/g	Time after spike, hrs.	Decay corrected count rate, cpm/g
37869	305	100	10.8	2086.889	3.38	2091.472
30172	305	100	10.6	1690.585	4.83	1695.893
22049	323	100	10.8	1207.000	9.83	1214.725
6872	319	100	10.9	360.716	19.76	365.371
4962	347	100	10.7	258.785	25.47	263.098
3695	365	100	10.9	183.303	51.98	189.592
2982	376	100	10.9	143.450	71.83	150.295
1487	344	100	10.8	63.500	122.53	68.756
1045	403	100	11.0	35.018	144.38	38.458
1119	317	100	11.0	43.745	196.98	49.711
665	221	100	11.0	24.218	267.08	28.802
2561	838	400	10.8	23.931	314.72	29.354
2943	972	400	10.9	27.124	387.97	34.890
3146	1897	400	10.9	17.188	435.63	22.804
2366	822	400	10.9	21.248	480.02	29.014
1843	833	400	10.8	14.028	509.73	19.528
<hr/>						
26944	305	100	13.0	1229.492	4.45	1233.048
35387	323	100	13.5	1558.400	10.17	1568.720
2477	375	100	13.2	95.545	29.03	97.363
1794	468	100	13.1	60.733	43.81	62.484
2282	426	100	13.3	83.729	48.11	86.385
1853	365	100	13.3	67.128	50.75	69.376
1215	365	100	13.1	38.931	52.22	40.273
1253	416	100	13.0	38.631	67.48	40.360
1378	376	100	13.2	45.545	71.12	47.697
953	337	100	13.3	27.789	99.92	29.651
1060	406	100	13.3	29.504	148.75	32.494
612	374	100	13.1	10.901	170.78	12.178
543	316	100	13.7	9.942	187.87	11.231
665	281	100	13.0	17.723	212.43	20.343
457	218	100	13.4	10.701	237.52	12.485
2206	1162	400	13.1	11.954	291.17	14.441
2150	1397	400	13.2	8.557	337.67	10.653
1841	843	400	13.5	11.089	360.67	14.014
2536	2057	400	13.8	5.207	430.20	6.883
1368	822	400	13.8	5.935	479.58	8.102
1411	802	400	13.5	6.767	523.33	9.503
<hr/>						
3676	347	100	26.3	75.947	23.88	77.133

Appendix Table 6 (Continued). Cockle sample count rate data.

Cs+b	Cb	Count time, sec	Net wt., g(1)	Count rate cpm/g	Time after spike, hrs.	Decay corrected count rate, cpm/g
31238	305	100	29.8	622.812	2.95	624.006
14134	319	100	30.6	270.882	19.52	274.336
7844	347	100	30.0	149.940	24.83	152.376
6718	347	100	29.7	128.707	25.90	130.889
4918	375	100	29.8	91.470	28.47	93.176
5535	426	100	33.3	92.054	47.62	94.944
5364	365	100	30.2	99.318	51.05	102.664
4014	376	100	29.8	73.248	71.35	76.720
2209	337	100	30.2	37.192	99.67	39.677
2513	336	100	29.8	43.832	119.22	47.358
1930	373	100	30.2	30.934	139.60	33.867
2122	374	100	30.9	33.942	171.53	37.939
1907	308	100	30.0	31.980	193.75	36.265
1313	296	100	30.0	20.340	218.77	23.443
871	223	100	30.6	12.706	243.67	14.883
1212	221	100	30.1	19.754	266.78	23.488
1099	271	100	30.3	16.396	286.38	19.745
900	223	100	31.3	12.978	332.35	16.102
900	216	100	30.6	13.412	360.92	16.952
839	269	100	31.0	11.032	406.98	14.367
892	192	100	31.2	13.462	454.15	18.076
690	219	100	30.1	9.389	509.17	13.065
<hr/>						
92099	305	100	55.9	985.267	5.50	988.790
147494	323	100	55.6	1588.176	8.43	1596.889
92980	323	100	55.9	994.530	9.25	1000.518
30385	393	100	55.8	322.495	55.98	334.427
15900	416	100	55.9	166.197	67.80	173.673
13596	351	100	55.8	142.419	75.88	149.609
12973	336	100	56.4	134.436	118.88	145.219
7685	364	100	55.5	79.146	125.43	85.858
4960	316	100	57.3	48.628	188.13	54.943
5978	281	100	55.9	61.148	212.05	70.171
5343	337	100	56.8	52.880	237.27	61.684
3524	221	100	56.0	35.389	267.27	42.093
2595	310	100	59.9	22.888	291.62	27.657
2412	221	100	50.0	26.292	315.10	32.258
<hr/>						
128232	305	100	56.3	1363.343	5.98	1368.644
6071	468	100	56.3	59.712	44.00	61.442
6418	426	100	56.0	64.200	47.13	66.194
3906	376	100	55.7	38.025	71.62	39.834

Appendix Table 6 (Continued). Cockle sample count rate data.

Cs+b	Cb	Count time, sec	Net wt., g(1)	Count rate cpm/g	Time after spike, hrs.	Decay corrected count rate, cpm/g
1934	373	100	56.5	16.577	91.60	17.592
3424	344	100	56.4	32.766	122.22	35.471
3101	403	100	56.2	28.804	144.50	31.636
1978	411	100	57.8	16.266	165.93	18.116
1757	281	100	57.6	15.375	218.20	17.714
1653	223	100	55.8	15.376	245.57	18.033
1057	271	100	57.5	8.202	286.68	9.879
938	223	100	56.9	7.540	306.83	9.201
1179	215	100	55.8	10.366	337.30	12.902
868	201	100	56.4	7.096	356.22	8.941
969	236	100	56.5	7.784	380.35	9.964
913	312	100	56.0	6.439	430.03	8.512
920	196	100	57.4	7.568	479.35	10.330
760	219	100	55.7	5.828	509.50	8.112
741	212	100	56.5	5.618	522.75	7.887
<hr/>						
134462	305	100	74.8	1076.126	5.02	1079.637
10944	375	100	74.5	85.119	27.98	86.679
11327	393	100	74.9	87.589	56.43	90.856
4551	337	100	75.4	33.533	100.35	35.790
4023	406	100	76.2	28.480	149.08	31.374
3019	411	100	76.3	20.509	166.17	22.844
2562	308	100	75.4	17.936	193.95	20.342
1967	221	100	74.6	14.043	266.83	16.698
1682	271	100	74.8	11.318	286.58	13.632
1683	266	100	75.6	11.246	306.63	13.722
1474	223	100	75.8	9.902	332.15	12.285
1777	201	100	75.5	12.525	356.05	15.780
1507	243	100	75.4	10.058	388.20	12.940
1551	269	100	75.7	10.161	407.13	13.234
2003	557	100	75.5	11.491	430.35	15.194
<hr/>						
60728	305	100	83.7	433.140	2.53	433.852
46144	347	100	85.4	321.759	24.30	326.873
7799	376	100	83.6	53.275	70.80	55.780
3797	364	100	84.2	24.463	125.76	26.544
2608	373	100	84.0	15.964	139.33	17.475
2618	374	100	85.0	15.840	171.32	17.703

Appendix Table 6 (Continued). Cockle sample count rate data.

Cs+b	Cb	Count time, sec	Net wt., g(1)	Count rate cpm/g	Time after spike, hrs.	Decay corrected count rate, cpm/g
38124	305	100	107.8	210.495	1.88	210.752
46350	426	100	107.9	255.370	47.82	263.420
39947	365	100	106.7	222.579	51.75	230.182
17975	351	100	107.5	98.367	76.15	103.350
13803	373	100	108.6	74.199	91.27	78.727
9671	403	100	108.6	51.204	144.03	56.222
5768	411	100	108.6	29.597	165.65	32.956
6598	308	100	107.1	35.238	193.25	39.947
5296	296	100	108.8	27.574	218.65	31.778
5349	223	100	108.1	28.451	243.93	33.332
4872	310	100	108.0	25.344	291.47	30.622
3897	221	100	107.7	20.479	315.18	25.127
3175	236	100	108.7	16.223	380.10	20.761
2825	269	100	109.1	14.057	407.28	18.310
2385	192	100	108.0	12.183	453.95	16.358
3282	196	100	109.6	16.894	479.92	23.068
1859	219	100	107.1	9.188	509.65	12.790
2439	212	100	107.6	12.418	523.50	17.443

Appendix Table 7. Retention experiment sample data.

Type of sample	Cs+b	Cb	Count time, sec	Net wt., g	Count rate cpm/g	Time after spike, hrs.	Gross count rate, cpm	Decay corrected count rate, cpm/g
Sediment	1364	936	400	96.4	0.666	267.15	64.20	0.792
	1297	1162	400	78.4	0.258	291.65	20.25	0.312
	1054	838	400	74.3	0.436	314.97	32.40	0.535
Water	1336	936	400	17.8	3.371	267.32	60.00	4.009
	1261	1162	400	13.1	1.134	291.50	14.85	1.370
	1007	838	400	15.8	1.604	315.00	25.35	1.968

Appendix Table 8. Bent-nose clam sample count rate data.

Cs+b	Cb	Count time, sec	Net wt., g(1)	Count rate cpm/g	Time after spike, hrs.	Decay corrected count rate, cpm/g
556	365	100	69.1	1.658	50.60	1.714
463	351	100	69.4	0.968	76.27	1.017
534	364	100	70.4	1.449	125.57	1.572
400	374	100	69.4	0.225	171.78	0.251
394	223	100	69.5	1.476	245.75	1.732
2304	1397	400	70	1.944	337.9	2.420
1315	802	400	69.5	1.107	523.75	1.555

Appendix Table 9. Tissue distribution sample count rate data.

Type of sample	Cs+b	Cb	Count time, sec	Net wt., g	Count rate cpm/g	Time after spike, hrs.	Time after spike counted, hrs	Gross count rate, cpm	Decay corrected count rate, cpm/g
Whole-body	3649	340	200	17.2	57.715	23.97	766.42	992.70	58.620
	4591	340	200	53.2	23.972	171.13	766.80	1275.30	26.788
	2898	340	200	35.3	21.739	237.88	766.53	767.40	25.369
	1736	340	200	47.7	8.780	430.47	766.63	418.80	11.610
Pallial Fluid	1606	833	400	5.2	22.298	23.97	601.63	115.95	22.648
	1572	708	400	17.0	7.624	171.13	602.00	129.60	8.519
	2392	708	400	12.1	20.876	237.88	601.75	252.60	24.361
	2172	708	400	19.6	11.204	430.47	601.87	219.60	14.815
Muscular Foot	676	340	200	1.1	91.636	23.97	768.52	100.80	93.073
	501	340	200	2.2	21.955	171.13	767.47	48.30	24.534
	608	340	200	1.4	57.429	237.88	768.20	80.40	67.016
	370	340	200	1.6	5.625	430.47	767.85	9.00	7.438
Visceral Mass	1243	340	200	1.0	270.900	23.97	768.72	270.90	275.147
	2462	340	200	4.7	135.447	171.13	767.55	636.60	151.358
	1447	340	200	2.0	166.050	237.88	768.42	332.10	193.771
	819	340	200	4.8	29.938	430.47	768.12	143.70	39.587

Appendix Table 9 (Continued). Tissue distribution sample count rate data.

Type of sample	Cs+b	Cb	Count time, sec	Net wt., g	Count rate cpm/g	Time after spike, hrs.	Time after spike counted, hrs	Gross count rate, cpm	Decay corrected count rate, cpm/g
Gills & Other Flesh Materials	1173	340	200	1.3	192.231	23.97	768.60	249.90	195.245
	994	340	200	4.8	40.875	171.13	767.63	196.20	45.677
	721	340	200	2.2	51.955	237.88	768.28	114.30	60.628
	531	340	200	4.9	11.694	430.47	767.98	57.30	15.463
Valves	709	340	200	13.7	8.080	23.97	768.67	110.70	8.207
	1059	340	200	41.2	5.235	171.13	767.72	215.70	5.850
	728	340	200	29.0	4.014	237.88	768.35	116.40	4.684
	616	340	200	35.9	2.306	430.47	768.03	82.80	3.050